

**Polymer Submicron- and Nano-Fibers:  
Applications in Healthcare, Drug delivery, Oil Spill Remediation and Print Transfer**

Shital Yadav

A Dissertation Submitted to  
Indian Institute of Technology Hyderabad  
In Partial Fulfillment of the Requirements for  
The Degree of Master of Technology



भारतीय प्रौद्योगिकी संस्थान हैदराबाद  
Indian Institute of Technology Hyderabad

Department of Chemical Engineering

June, 2015

## DECLARATION

I declare that this written submission represents my ideas in my own words, and where others' ideas or words have been included, I have adequately cited and referenced the original sources. I also declare that I have adhered to all principles of academic honesty and integrity and have not misrepresented or fabricated or falsified any idea/data/fact/source in my submission. I understand that any violation of the above will be a cause for disciplinary action by the Institute and can also evoke penal action from the sources that have thus not been properly cited, or from whom proper permission has not been taken when needed.

*Shital Yadav*

---

SHITAL YADAV

CH13M1012

## APPROVAL SHEET

This thesis entitled **Polymer Submicron- and Nano-Fibers: Applications in healthcare, drug delivery, oil spill remediation and print transfer technique** by **Shital Yadav** is approved for the degree of Master of Technology from IIT Hyderabad.



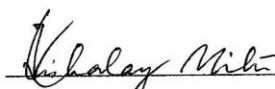
---

Dr. Mudrika Khandelwal  
Dept. of Material Science and Metallurgical Engg.



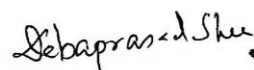
---

Dr. Saptarishi Majumdar  
Dept. of Chemical Engineering



---

Dr. Kishalay Mitra  
Dept. of Chemical Engineering



---

Dr. Debaprasad Shee  
Dept. of Chemical Engineering



---

Dr. Chandra Shekhar Sharma  
Dept. of Chemical Engineering  
Adviser

## ACKNOWLEDGEMENTS

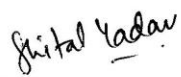
I would like to express my gratitude to my supervisor **Dr. Chandra Shekhar Sharma** who has been an exceptional mentor and constant source of inspiration for me; exceptional mentor because he has always steered me in the right direction, afforded me the freedom of thought and flexibility of working at odd hours, and always found time from his busy schedule to discuss my problems. He has been a constant source of inspiration because of his originality of thought in research and work ethic. I am indebted to him for all the help and outstanding ideas, he has given me during the course of this work.

I am extremely thankful to **Anindita Laha** and **Mani Pujitha Illa** for their help and support in research work. I thank **Manohar Kakunari** and **Utkarsh Bhutani** for teaching me many protocols and instruments used for my work. I appreciate help provided by **Rajendar Bandaru** Sir in completion of my work.

I have been extremely fortunate to have shared the lab space with my colleagues in Dr. Sharma's research group. I specially acknowledge **M.G. Karthik, Srinadh Mattaparthi and Akanksha Adaval**. I also cherish the time spent with **Rishabh Saraswat, Aditaya Aagare, Shubham Kaushik, Jaya Sanjana, Akash Nathani, Suresh Mamidi and Anulekha Haridas**.

We acknowledge **Indian Institute of Technology Hyderabad** for providing necessary research infrastructure to carry out this work. I will fail in my duties if I don't mention **Dr. Saptarishi Majumdar, Dr. Kishalay Mitra** and **Dr. Mudrika Khandelwal** for their encouragement, insightful comments and suggestions in the work.

That finally brings me to the pleasant task of formally thanking my family members. I cannot express in words my appreciation for my **parents** and for everything that they have done for me. I thank my brother **Vikas** from bottom of my heart for just being there when I needed him the most. Last but not the least, I would like to thank the almighty God who provided me the strength to work.

  
**SHITAL YADAV**

*Dedicated to*

*My parents*

## NOMENCLATURE

AUL	Absorbency under load
BET	Brunauer-Emmett-Teller
BL	Bottom layer
CA	Cellulose acetate
CA10	Cellulose Acetate with 10wt% SPA
CA5	Cellulose Acetate with 5wt% SPA
DMA	N,N-dimethylacetamide
FESEM	Field emission scanning electron microscope
FTIR	Fourier transform infrared spectroscopy
GCMS	Gas chromatography- mass spectroscopy
GI	Gastrointestinal tract
GNF	Gelatin nanofibers
G-PNF	Piperine loaded gelatin nanofibers
GTA	Glutaraldehyde
ML	Middle layer
PE	Primary extract
PEF	Fibers prepared using primary extract
PS	Polystyrene
PSF	Electrospun polystyrene fibers
SAP	Super-absorbent polymer
SEM	Scanning electron microscope
SPA	Sodium-polyacrylate
TGA	Thermogravimetric analysis
TL	Top layer
TLF	Fibers prepared using top layer

## LIST OF TABLES

<b>Table 2.1</b>	List of commercial female hygiene product of various categories considered in this work as reference	<b>10</b>
<b>Table 2.2</b>	Process parameters optimized for electrospinning in this work. 'A' represents cellulose acetate solution and 'B' and 'C' represent 5% (w/v) and 10 % (w/v) solutions of SPA respectively	<b>12</b>
<b>Table 3.1</b>	Summary of degradation study for GNF and G-P NF crosslinked over different time interval, in dissolution medium of different pH	<b>33</b>
<b>Table 4.1</b>	Properties of top and bottom layer of PE	<b>49</b>
<b>Table 5.1</b>	Properties of mustard oil and coconut oil	<b>59</b>

## LIST OF FIGURES

<b>Figure 1.1</b>	Applications of polymer nanofibers	<b>3</b>
<b>Figure 2.1</b>	Schematic of electrospinning set-up used in this work	<b>11</b>
<b>Figure 2.2</b>	Test setup used to determine absorbency under load	<b>13</b>
<b>Figure 2.3</b>	(a) SEM image of commercial sample, S1 and FESEM images of electrospun fibers of (b) CA (c) CA5 and (d) CA10.	<b>15</b>
<b>Figure 2.4</b>	Free absorbency test in (a) distilled water (b) saline solution (c) synthetic urine and (d) equilibrium absorbency for all samples (electrospun nanofibers CA, CA5 and CA10 and all six commercial samples)	<b>17</b>
<b>Figure 2.5</b>	Absorbency under load in saline solution for electrospun nanofibers samples and commercial samples (S1, S2, S3 and S4)	<b>19</b>
<b>Figure 2.6</b>	Pictorial representation of the absorbent cores of commercial samples (a) S1 (b) S2 (c) S5 (d) S4 and electrospun CA nanofibers (e). Figure a'-e' shows the changes after dipping in distilled water for 10 minutes in respective samples	<b>21</b>
<b>Figure 2.7</b>	Residue test for electrospun fiber samples (CA and CA5) and commercial samples (S1 and S2)	<b>22</b>
<b>Figure 2.8</b>	Young's Modulus for different samples (electrospun CA nanofibers and commercial samples S1, S2, S4 and S5)	<b>22</b>
<b>Figure 3.1</b>	Digital images representing, (a) effect of crosslinking for 6 min on GNF (b) completely degraded (c) partially degraded and (d) intact membrane	<b>32</b>
<b>Figure 3.2</b>	FESEM images of (a) as-spun GNF, (b) GNF after crosslinking with GTA vapor for 6 min, (c) as-spun G-P NF, and (d) G-P NF after crosslinking with GTA vapor for 6 min	<b>34</b>



<b>Figure 3.3</b>	Effect of crosslinking on (a) GNF and (b) G-P NF ; (c) stability of piperine (d) chemical structure of piperine used as a drug	<b>35</b>
<b>Figure 3.4</b>	Thermogram of as-spun and 6 min crosslinked GNF membrane	<b>36</b>
<b>Figure 3.5</b>	Cumulative release of piperine for (a) 4 min (b) 6 min and (c) 8 min crosslinked G-P NF in different pH (1.2, 6, 7.4 and 8)	<b>37</b>
<b>Figure 3.6</b>	Cumulative release of piperine for different crosslinking time in (a) pH 1.2. (b) pH 6 (c) pH 7.4, and (d) pH 8	<b>39</b>
<b>Figure 4.1</b>	Steps for preparing primary extract from the orange peel (a-d); layers in primary extract (e)	<b>46</b>
<b>Figure 4.2</b>	(a) template and print transfer using orange peel extract (b-f) on paper	<b>47</b>
<b>Figure 4.3</b>	(a) Gas chromatograph of TL, (b) Identified components corresponding to each peak in gas chromatograph	<b>48</b>
<b>Figure 4.4</b>	Print transfer on substrates (a) paper (b) cotton cloth (c) skin and (d) nail	<b>50</b>
<b>Figure 5.1</b>	Materials required (a) and steps of drawing fibers from geometric scale (b-h); fibers aligned at 90 <sup>0</sup> (i) and 45 <sup>0</sup> (j)	<b>57</b>
<b>Figure 5.2</b>	(a) Fibers between hand and scale, (b) degradation of scale after deposition, (c) fibers from thermocol, (d) degradation of thermocol; ways of peel orange (e-f)	<b>61</b>
<b>Figure 5.3</b>	Digital images of (a) PEF and (b) TLF; SEM images of PEF (c) and (d); SEM images of (e) TLF and (f) PSF	<b>62</b>
<b>Figure 5.4</b>	FTIR analysis of TLF, PSF and PEF	<b>63</b>
<b>Figure 5.5</b>	XRD analysis of PSF and PEF	<b>64</b>
<b>Figure 5.6</b>	(a) Optical image of water and oil droplet on as-drawn PEF and (b) contact angle on PEF	<b>65</b>
<b>Figure 5.7</b>	TGA curve of TLF,PSF and PEF	<b>65</b>

<b>Figure 5.8</b>	Absorption capacity of PEF, TLF and PSF in coconut and mustard oil	<b>66</b>
<b>Figure 5.9</b>	Oil retention capacity of PEF, TLF and PSF in (a) coconut oil (b) mustard oil and respective percent retention (a' and b')	<b>67</b>
<b>Figure 5.10</b>	Reusability of (a) PEF and (b) TLF in coconut and mustard oil	<b>68</b>
<b>Figure 5.11</b>	Clean-up of mustard oil by PEF in static system (a-c) and dynamic system (d-f)	<b>69</b>
<b>Figure 6.1</b>	Steps in making yarn and coil (a-e) ; SEM images of (f) yarn and (g) coil	<b>75</b>
<b>Figure 6.2</b>	Knotted structures (a) square, (b)overhand and (c) weaver's knot; (d) coils after opening knot and (e) weaving different diameter coils	<b>75</b>
<b>Figure 6.3</b>	Use of eraser for fabricating fibers	<b>76</b>
<b>Figure 6.4</b>	Digital images of steps of working set-up.	<b>78</b>

## **Scientific Contribution from This Work**

### **Patents:**

#### **International:**

1. PCT Application No. PCT/IB2015/000829, Date of Filing: June 01, 2015

(Process of Fabrication of Natural Sub-micron Aligned Fibers with Controllable Geometry from a Citrus Peel Extract)

#### **Indian:**

2. Indian Patent Application No. 3684/CHE/2014, Date of Filing: July 28, 2014.

(Cellulose Acetate based Non-woven Nano-fiber Matrix with High Absorbency Properties for Female Hygiene)

3. Indian Patent Application No. 5928/CHE/2014, Date of Filing: November 26, 2014

(Process of Fabrication of Natural Sub-micron Aligned Fibers with Controllable Geometry from a Citrus Peel Extract)

### **International Peer-Reviewed Journal Publications:**

#### **Under Review:**

1. Anindita Laha; Shital Yadav; Sapatrsi Majumdar and Chandra S. Sharma. In-Vitro Release Study of Hydrophobic Drug using Electrospun Cross-linked Gelatin Nanofibers, Biochemical Engineering Journal.

2. Shital Yadav, Illa Manipujitha, Tulika Rastogi and Chandra S. Sharma. High Absorbency Cellulose Acetate Electrospun Nanofibers for Feminine Hygiene Application, ACS Applied Materials and Interfaces.

#### **Under Preparation:**

3. Shital Yadav, Mudrika Khandelwal, Saptarshi Majumdar and Chandra S. Sharma. Orange Peel Extract: A Wonderful Engineering Material.

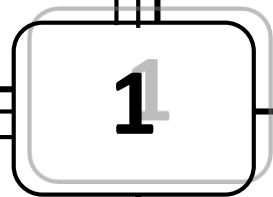
## TABLE OF CONTENTS

Declaration	i
Approval sheet	ii
Acknowledgements	iii
<b>Nomenclature</b>	<b>v</b>
<b>List of tables</b>	<b>vi</b>
<b>List of figures</b>	<b>vii</b>
<b>Scientific contribution</b>	<b>X</b>
<b>1. Introduction</b>	<b>1</b>
1.1 Background	2
1.2 Objective and Layout of thesis	3
References	5
<b>2. High Absorbency Cellulose Acetate Electrospun Nanofibers for Feminine Hygiene Applications</b>	<b>6</b>
Abstract	7
2.1 Introduction	8
2.2 Experimental Methods	9
2.3 Results and Discussion	14
2.4 Conclusions	23
2.5 Acknowledgements	23
References	24
<b>3. <i>In-vitro</i> Release Study of Hydrophobic Drug using Electrospun Cross-linked Gelatin Nanofibers</b>	<b>26</b>
Abstract	27
3.1 Introduction	28
3.2 Experimental Methods	29
3.3 Results and Discussion	32
3.4 Conclusions	39
3.5 Acknowledgements	39
References	40

<b>4. Orange Peel Extract as Natural Transfer Solution for Print Transfer</b>	<b>43</b>
<b>Technique</b>	
Abstract	<b>44</b>
4.1 Introduction	<b>45</b>
4.2 Experimental Methods	<b>46</b>
4.3 Results and Discussion	<b>48</b>
4.4 Conclusions	<b>50</b>
4.5 Acknowledgements	<b>51</b>
References	<b>52</b>
<b>5. Recycled Polystyrene based Submicron, Aligned Fibers using Orange Peel Extract for Oil Spill Remediation</b>	<b>53</b>
Abstract	<b>54</b>
5.1 Introduction	<b>55</b>
5.2 Experimental Methods	<b>55</b>
5.3 Results and Discussion	<b>60</b>
5.4 Conclusions	<b>69</b>
5.5 Acknowledgements	<b>70</b>
References	<b>71</b>
<b>6. Staple Spun Yarn from As-drawn Fibers from Polystyrene Waste and Scale-up of Recycling process</b>	<b>72</b>
Abstract	<b>73</b>
6.1 Introduction	<b>74</b>
6.2 Experimental Methods	<b>74</b>
6.3 Results and Discussion	<b>77</b>
6.4 Conclusions	<b>79</b>
6.5 Acknowledgements	<b>79</b>
References	<b>80</b>
<b>7. Summary and Future Directions</b>	<b>81</b>
7.1 Summary	<b>82</b>
7.2 Future directions	<b>82</b>



# Introduction



## 1.1 Background

A polymer is a long chain molecule, made up of repeated units called monomers.<sup>1</sup> They are classified as natural or synthetic polymers. Natural polymers occur in nature and can be extracted, for examples silk, wool, DNA, cellulose, proteins etc. Synthetic polymers are derived from petroleum oil, and made by scientists and engineers. Examples of synthetic polymers include nylon, polyethylene, polyester, Teflon, and epoxy.<sup>2</sup> There are different forms in which a material or polymer can be used such as films, particles, micro- or nano-fibers, gels<sup>1</sup> etc. Among these, nanofibers have an advantage of having high surface to volume ratio and high porosity and therefore preferred in many applications.<sup>1</sup>

A fiber can be defined as one dimensional threadlike structure, having certain diameter and length<sup>1</sup>. However, for real applications, they have to exhibit certain properties such as mechanical, optical, electrical, thermal etc., depending upon its function. For example, in textiles, fibers should have good mechanical properties like strength, elasticity etc. enabling it to withstand weaving, knitting or other textile deformations.<sup>3</sup> These properties can be achieved by selecting appropriate material and fiber preparation technique.

Depending upon the end-product specifications or applications, different techniques can be used to make fibers. Some of the techniques are listed as follows<sup>1</sup>:

- (i) drawing wherein fibers are drawn while polymer is still solidifying
- (ii) electro spinning wherein it uses electrically charged jet of polymer solution to make fibers
- (iii) wet spinning wherein polymer solution is extruded in precipitating liquid to get fibers
- (iv) dry spinning wherein solidification is achieved by evaporating the solvent in a stream of air or inert gas
- (v) melt spinning uses polymer melt to pass through spinneret
- (vi) template synthesis implies the use of template or mold to get desired shape of a product
- (vii) phase separation is based on the separation of phases due to physical incompatibility
- (viii) self-assembly refers to building up of nanoscale fibers using smaller molecules as building blocks.

Micro- or nano-fibers, as mentioned above, can be produced by many techniques and are advantageous over other forms in which polymers are used. As a result, fibers are prevailing in areas such as healthcare, energy and environment.<sup>1</sup> Also, nanofibers are gaining popularity as



carrier for drug, protecting drug from the bloodstream and releasing it at the targeted site. Figure 1.1 shows different application areas of polymer nanofibers varying from sensors, filtration, electronics to tissue engineering and military protection clothing.

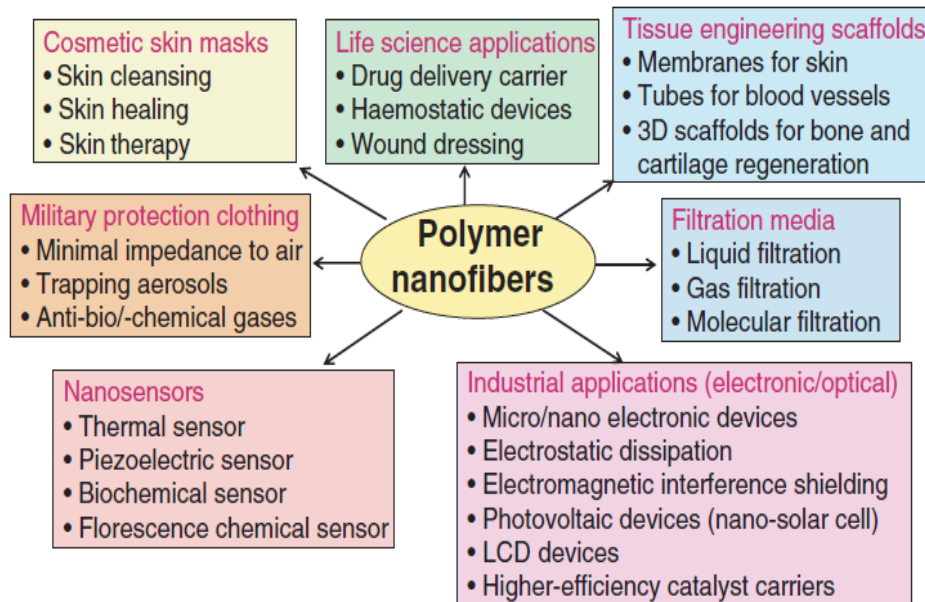


**Figure 1.1** Applications of polymer nanofibers<sup>4</sup>

Natural fibers such as wool, cotton, silk etc. are readily used in healthcare from decades. Nowadays, less expensive, more easily cleanable man-made fibers such as rayon, and synthetic fibers such as nylon, polyester, etc. are replacing them.<sup>5</sup> However, synthetic fibers are non-biodegradable and contributes to pollution in environment. As a result, different techniques were developed in order to recycle them depending upon polymer properties. Greener technologies are more popular, for example Shin et. al<sup>6</sup> used d-limonene as solvent to dissolve expanded polystyrene and fabricated electrospun nanofibers from it. These fibers can then be used in different applications.

## 1.2 Objective and layout of thesis

The primary motivation of this thesis is to fabricate micro- and nanofibers using biopolymers and using them for different applications. The following are the primary objectives of this work:

- A. Use of biocompatible, biodegradable polymers such as cellulose acetate and gelatin for fabrication of fibers
- B. Using electrospun nanofibers as drug carrier and sanitation purposes

- C. Developing a novel method in order to recycle polystyrene waste into aligned sub-micron fibers
- D. Exploring applications of prepared recycled polystyrene fibers in textiles and oil spill remediation

We start with fabricating nanofibers of biopolymer cellulose acetate by electrospinning in chapter 2. These fibers were then encapsulated with super absorbent polymer such as sodium polyacrylate and the effect of encapsulation was studied. Further, the prepared non-woven nanofibrous mat of cellulose acetate (CA) with or without superabsorbent polymer was tested for application in feminine hygiene products.

The next chapter (chapter 3) presents the synthesis of gelatin nanofibers by electrospinning. Gelatin nanofibers are hydrophilic in nature and therefore dissolves when comes in contact with water. Therefore, to use gelatin nanofibers, they were crosslinked as mentioned in the chapter. These prepared gelatin nanofibers were then used as the drug carrier in oral drug delivery by encapsulating piperine, as the model drug. We further discuss the stability and release of drug from carrier.

Chapter 4 reports a novel way of using waste orange peels. In this chapter we demonstrates the preparation of extract from orange peel by very easy and inexpensive method, followed by using it as a natural transfer solution for print transfer method.

In chapter 5 we report here novel and innovative way of producing sub-micron, aligned fibers from objects made up of polystyrene, with controllable geometry, from extract obtained from peel of orange fruit. The process depicted here for the fabrication is not only facile, flexible but at the same time versatile with minimum requirements for making aligned fibers. These fibers were then used as sorbent material in case of oil spills.

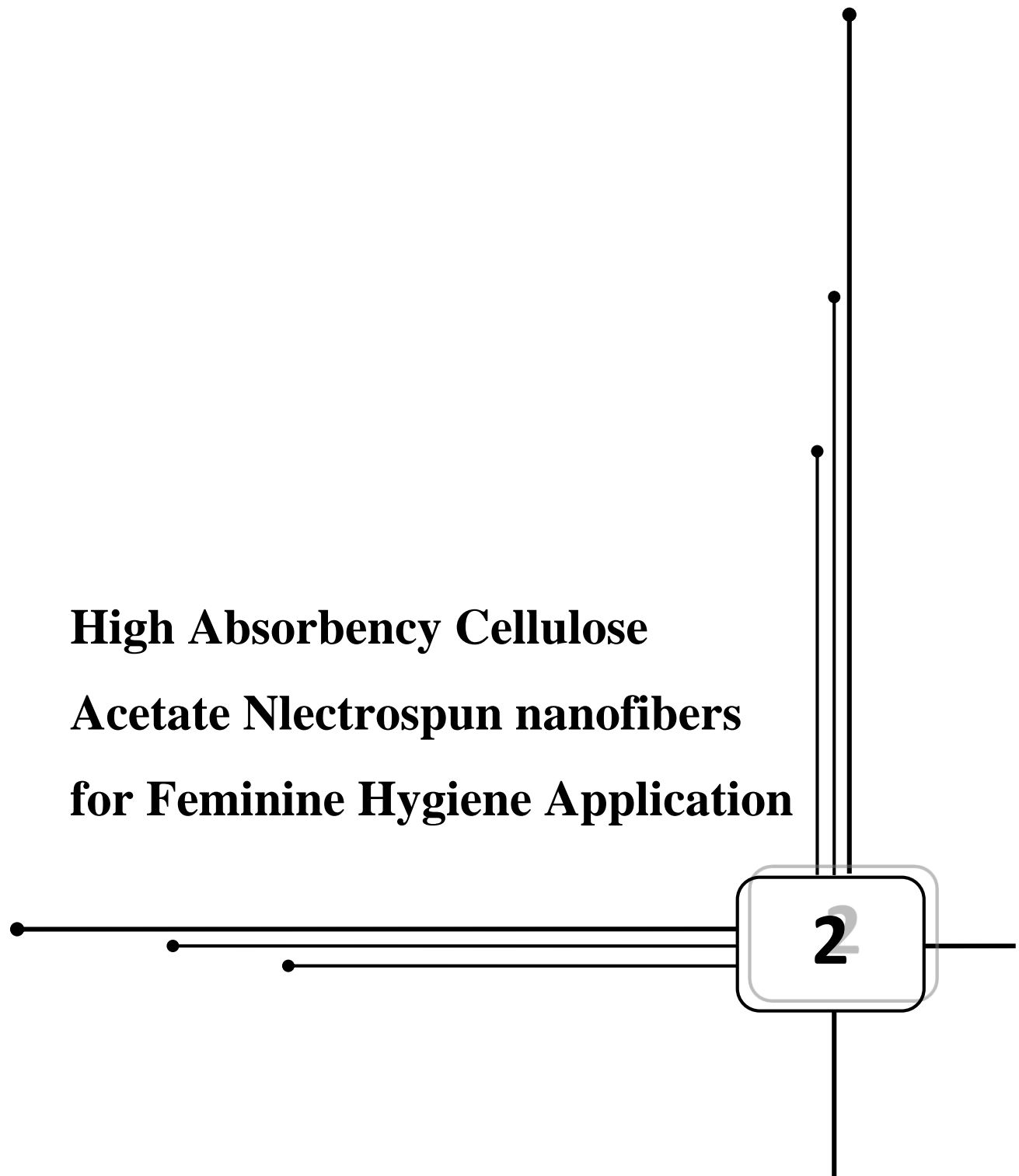
The prepared as-drawn polystyrene fibers were then tested for use in textile fabric. For this, the fibers were converted in to yarns and coils as explained in chapter 6. Having developed a method for recycling of waste polystyrene into fibers and successfully tested for oil clean up and textiles application, next step is to make set-up to overcome some limitations of the method. Therefore, second part of chapter 6 demonstrates the set-up replicating the method.

The final chapter (chapter 7) is dedicated to the conclusions made from the work presented in this thesis. We also propose some future directions based on the work carried out.

## References

1. S. Ramakrishna, K. Fujihara, W.E. Teo, T.C. Lim, Z. Ma, An Introduction to Electrospinning and Nano-fibers, World Scientific Publishing Co. Pte. Ltd.2005
2. Website: <http://www.cmu.edu/gelfand/k12-teachers/polymers/natural-synthetic-polymers/>
3. C. A. Lawrence, Fundamentals of spurn yarn technology, CRC press, 2003.
4. C. Burger, S. H. Benjamin, C. Benjamin, Nanofibrous materials and their applications, Annu. Rev. Mater. 36 (2006),333–368.
5. The future of fabric-healthcare, website: <http://www.noharm.org/us>
6. C. Shin, G. G. Chase, Nanofibers from recycle waste expanded polystyrene using natural solvent, Polymer Bulletin 55 (2005), 209–215

**High Absorbency Cellulose  
Acetate Nlectrospun nanofibers  
for Feminine Hygiene Application**



## **Abstract**

We have electrospun cellulose acetate (CA) with or without superabsorbent polymer i.e., sodium polyacrylate (SPA) in the form of non-woven nanofibrous mat and successfully demonstrated their application in feminine hygiene products. Surface morphology and specific surface area for these electrospun CA nanofibrous mat with and without SPA were studied using FESEM and BET adsorption method. Further to investigate their absorbent properties, free absorbency at different time intervals and equilibrium absorbency were measured in distilled water, saline solution (0.9 wt. % NaCl) and synthetic urine respectively. Absorbency under load was also tested in saline solution for practical use. The amount of residue and tensile properties were determined for these electrospun CA based nanofibrous mats to enable their use as absorbent core in female hygiene products. While comparing all these results with six different types of commercially available feminine sanitary napkins which are primarily composed of micron sized cellulosic fibers with superabsorbent polymers in the form of granules or fabric, we found that pure CA electrospun nanofibers showed significantly higher absorbency in all conditions in all different mediums used. As concluded, use of electrospun CA nanofibers in place of micron size fabric in commercial female sanitary napkins not only enhances the absorption properties, mechanical strength and remarkably reduces residual percentage but also eliminates the use of SAP without compromising with their performance. This in turn may pave the way to resolve many health and environmental issues related with the use non-biodegradable SAP.

## 2.1 Introduction

Menstrual hygiene is an important issue for every woman, as poor menstrual hygiene increases the vulnerability towards reproductive tract infections (RTIs).<sup>1</sup> There are different types of feminine hygiene products commercially available such as sanitary napkins, tampons, panty shields, wipes and cosmetic removal pads. Among these, feminine sanitary pad/napkin is an important disposable absorbent hygiene product. Its functions are to absorb and retain menstrual fluid discharge and isolate it from skin, along with maintaining comfort, preventing odor and staying in place.<sup>2</sup> To accomplish all these requirements, sanitary pads constitutes different layers like cover stock, acquisition and distribution layer, absorbent core, back sheet, tissue, elastic wing and siliconised paper.<sup>2</sup> Absorbent core gives the desired absorption capacity to sanitary pads and is mainly made up of hydrophilic cellulosic fibers such as wood derived fluff pulp or viscose rayon.<sup>2</sup> As the diameter of these cellulosic fibers present in commercially available products is in range of few tens of microns, their absorption capacity is less owing to their lower surface area. To improve the absorption capacity, some of the commercially available female hygiene products use superabsorbent polymers (SAPs) either in the form of granules within cellulosic fiber matrix or in the form of composite fabric layer.<sup>2</sup>

SAPs are commonly divided into two main classes i.e., synthetic (petrochemical-based) and natural (polysaccharide- and polypeptide based).<sup>3</sup> Most of these superabsorbents are produced from acrylic acid, its salt and acrylamide.<sup>3</sup> The superabsorbents available in the market today are primarily based on cross- linked sodium polyacrylate (SPA) gels.<sup>2</sup> It facilitates in increasing the liquid absorption capacity and liquid retention capacity tremendously, thus allowing the product to be thinner but with improved performance.<sup>2</sup>

However, there are some harmful chemicals present in the commercially available sanitary napkins. For example, dioxins are used to bleach the cotton/material used for making absorbent core, but it is responsible for side effects in the body such as pelvic inflammatory disease, ovarian cancer, immune system damage, impaired fertility, diabetes, etc.<sup>4</sup> As mentioned above, SAPs are added to increase the absorption capacity, but in 1980s, use of SAPs was restricted in tampons due to its possible link with toxic shock syndrome, potentially fatal illness caused by a bacterial toxin.<sup>5</sup> Further as SAPs are petroleum based products and therefore does not degrade readily in landfills, their use is not eco-friendly as well.

Therefore the objective of this work is to minimize the use of SAPs in female hygiene products considering their possible adverse health effects. For this, we intend to fabricate cellulose based nanofibers and suggest their use as adsorbent core in female hygiene products. The increased specific surface area of nanofibers as compared to micron sized fibers present in commercial

products also justifies well this objective and may compensate for the absorption capacity while using SAPs.

Electrospinning is one of the simple and cost effective method used to synthesize fibers with diameter ranging from 10 nm to 10 $\mu$ m.<sup>6,7</sup> This method was invented by Formhals in 1934.<sup>8</sup> Electrospinning process uses high electric field as a driving force to draw fibers from electrically charged polymer solution or polymer melt.<sup>6-10</sup> Electrospun fibers possesses characteristics such as high surface-to-volume ratio, tunable porosity and flexible morphology with controllable diameter,<sup>11</sup> making them suitable for use in wide range of applications. Here as we discussed above, we primarily aim to exploit the large surface area of electrospun nanofibers in achieving the high absorption capacity.

In literature, cellulosic fibers have been used for absorption of water and other aqueous fluids.<sup>12</sup> However solvents used for cellulose, such as ionic liquids, are not completely volatile and require coagulation step to get stable fibers.<sup>12</sup> On the other hand, cellulose derivatives such as cellulose acetate, hydroxypropyl cellulose, hydroxypropyl methyl cellulose etc.,<sup>11-12</sup> can be easily dissolved in different volatile solvents that makes them suitable for electrospinning. Among these derivatives cellulose acetate is biocompatible, biopolymer which is easily available and has low cost.<sup>13</sup> It shows good hydrolytic stability and can be recycled in environment by biodegradation.<sup>14</sup> Therefore, we choose cellulose acetate as a material to prepare nanofabric mat for its use as an absorbent core.

In this article, electrospun nanofibers of cellulose acetate, with and without SPA encapsulation, were fabricated and characterized in terms of their surface morphology and mechanical properties. To demonstrate their use in female hygiene application, different tests such as free absorbency, equilibrium absorbency, absorbency under load and percentage residue were performed in different mediums i.e, distilled water, saline solution and synthetic urine respectively. The results obtained were then compared with some of the known commercially available feminine sanitary napkins.

## **2.2 Experimental Methods**

### **2.2.1 Materials**

Cellulose acetate ( $M_n$  29,000) and poly (acrylic acid sodium salt) ( $M_n$  5,100) were purchased from Sigma-Aldrich, India. Acetone (99% purity) and N, N-dimethylacetamide (99.5%) were received from Merck India. Distilled water from Millipore was used throughout the experiments. Six feminine hygiene commercial products namely, Whisper Choice, Whisper

Ultra Clean, Whisper Maxi-Fit, Whisper Maxi Nights, Stayfree Secure and Carefree panty liner were purchased from the local market.

### 2.2.2 Commercial feminine sanitary napkins as reference

There are several different types of disposable menstrual pads. They are classified on basis of their use in different conditions. We have considered six different commercial products (S1-S6) as summarized in Table 2.1.

**Table 2.1** List of commercial female hygiene product of various categories considered in this work as reference.

Sample Name	Commercial Product	Category	Conditions of Use
S1	Whisper Ultra Clean	Ultra-thin	Heavy flow
S2	Whisper Choice Ultra	Regular	Low to medium flow
S3	Stayfree Secure (Regular)	Regular	Low to medium flow
S4	Whisper Maxi-fit	Maxi / Super	Heavy flow
S5	Whisper Maxi nights	Overnight/ Maternity	Very heavy flow
S6	Carefree Panty Liner	Panty Liner	Daily flow

### 2.2.3 Synthetic urine preparation<sup>15</sup>

Synthetic urine was prepared by adding the following to distilled water to give a solution with a final volume of 1 litre: 25 g urea, 9 g sodium chloride, 2.5 g sodium phosphate, 3 g ammonium chloride, and 3 g sodium sulfite.

### 2.2.4 Polymer solution preparation with and without SAP

Cellulose acetate was dissolved in a mixture of acetone and N, N-dimethylacetamide (DMA) (2:1, v:v) to make 16 wt. % solution for electrospinning. The mixture was stirred to get a clear and transparent solution of cellulose acetate. In two other formulations, 5% (w/v) and 10% (w/v) solutions of sodium poly acrylate (SPA) were prepared by mixing SPA in methanol and then added to the above prepared cellulose acetate solution in 1:1 ratio. On adding SPA directly



to cellulose acetate solution, it agglomerated and therefore was not recommended for electrospinning.

### 2.2.5 Electrospinning

The basic setup of electrospinning consists of a syringe pump, voltage source and a collector. Figure 2.1 illustrates the schematic of electrospinning setup and process. Syringe pumps help in maintaining the desired flow rate. When sufficiently high voltage is applied to a liquid droplet, it becomes charged and electrostatic repulsion counteracts the surface tension, resulting in a change in shape of the droplet, known as the Taylor cone.<sup>10</sup> At this point, liquid erupts from the surface and fibers get deposited on the grounded collector. Polymer solution gets charged and internal repulsion led to instability in polymer jet, known as Rayleigh instability or whipping motion of the jet, depending on electric field strength.<sup>10</sup> Solvent evaporates in the distance between tip and collector and solidified deposition obtained on the collector. To get continuous uniform nanofibers or desired morphology, electrospinning parameters were optimized. These were feed rate, voltage applied, tip-to-collector distance and needle (tip) diameter. Table 2.2 summarizes the final parameters for preparing samples by electrospinning.

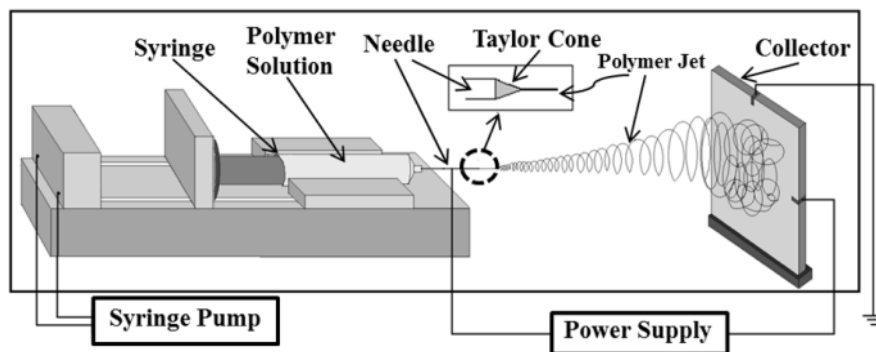


**Figure 2.1** Schematic of electrospinning set-up used

In this study, three different polymer solutions i.e., cellulose acetate (CA), cellulose acetate with 5 wt. % SPA (CA5) and cellulose acetate with 10 wt. % SPA (CA10), were used for electrospinning. Aluminum foil placed on the copper collector was used as substrate to deposit these electrospun fibers.

### 2.2.6 Morphological characterization

The surface morphologies of the electrospun nanofibers were observed by using field emission scanning electron microscopy (FESEM) (Carl Zeiss, SUPRA 40). Electrospun nanofibers were

removed from the aluminum foil and cut into small pieces of 1 x 1 cm<sup>2</sup>. All samples were sputtered with thin layer of gold before image analysis in FESEM in order to minimize the charge effect. For commercial products considered as reference, absorbent core was removed and then examined in scanning electron microscope.

**Table 2.2** Process parameters optimized for electrospinning in this work. ‘A’ represents cellulose acetate solution and ‘B’ and ‘C’ represent 5% (w/v) and 10 % (w/v) solutions of SPA respectively.

Polymer Solution	Applied Voltage (kV)	Flow rate (μl/min)	Needle diameter (gauge)	Distance (cm)
A	10	5	18	10
A:B = 1:1	12	10	18	10
A:C = 1:1	12	10	18	10

### 2.2.7 Specific surface area (SSA) measurement

The Brunauer–Emmett–Teller (BET) surface area of electrospun CA nanofibers with and without SPA and two different types of commercial samples was determined by N<sub>2</sub> physisorption using Quantachrome instruments v3.01. The weight of the sample was fixed to be 100 mg. All samples were degassed at 80<sup>0</sup> C for 60 min in nitrogen. The SSAs were determined by a multi-point BET measurement with nitrogen as the adsorbate.

### 2.2.8 Free absorbency test<sup>15</sup>

This test was done to quantify the absorption capacity of sample with respect to time, when allowed to swell freely. Electrospun nanofibers were removed from the aluminum foil to prepare free standing fabric mat. Similarly, absorbent core was removed from commercial products. These were then cut into approximately 2 x 2 cm<sup>2</sup> size and weighed, W<sub>1</sub> i.e., dry weight. The sample was then placed in a beaker containing distilled water and removed after 5 seconds. The excess water was allowed to drain off with help of tissue paper, for 30 seconds. The sample was weighed again, W<sub>2</sub> i.e., wet weight. This process was continued with measurements taken after immersion for 10, 20, 30, 60, 120 and 180 seconds respectively. Free absorbency can be calculated as:

$$Q = [(W_2 - W_1) / W_1] * 100$$

where Q = Percent free absorbency.

Similar procedure was followed to determine the free absorbency with 0.9 wt. % solution of sodium chloride i.e., saline solution and synthetic urine.

### 2.2.9 Equilibrium absorbency<sup>15</sup>

Free absorbency test carried out for time interval of 24 h to know the maximum absorption capacity of the sample is known as equilibrium absorbency. Solutions used are distilled water, saline solution and synthetic urine. Percentage equilibrium absorbency was calculated as follows

$$Q' = [(W2-W1)/W1] * 100$$

where, Q' = percent equilibrium absorbency

W1= Initial (dry) weight of the sample;

W2= final (wet) weight of the sample, after keeping immersed in solution for 24 h

### 2.2.10 Absorbency under load (AUL)<sup>3</sup>

This test was done to know the absorption capacity, if certain load is applied on the sample. By definition, this method is used to measure the ability of a superabsorbent to absorb 0.9 wt. % saline solution against certain pressure. In this study, it is used to measure the absorption capacity of electrospun nanofibers prepared and absorbent core of commercial samples in saline solution, when compressive load is applied while absorption. The setup for AUL tester as shown in Figure 2.2 contains a glass filter plate (d=30mm), placed in petri dish. A filter paper (d = 30mm) was placed on top of glass filter plate. Sample was cut in circular shape, with diameter of 30mm, and weighed (W1). Weight, 50 g/cm<sup>2</sup>, was kept on the assembly with help of cylindrical beaker and 0.9 wt. % of NaCl solution was poured in petri dish. Sample was removed after 60 min and weighed (W2).

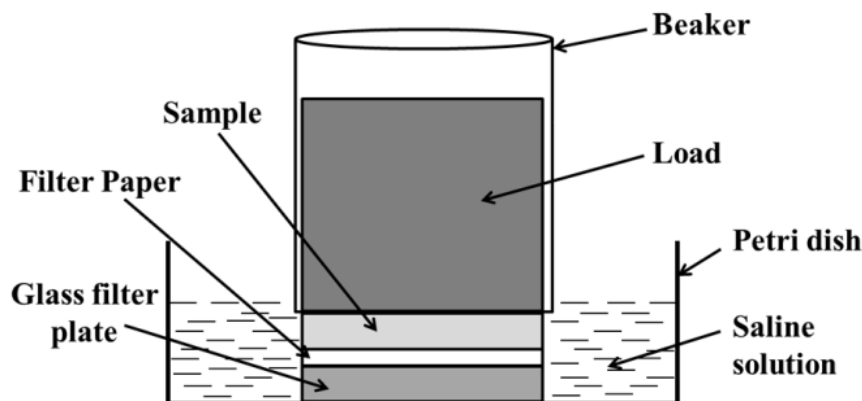


**Figure 2.2** Test setup used to determine absorbency under load.

Percentage absorbency under load will be given by:

$$Q'' = [(W2-W1)/W1] * 100$$

where  $Q''$  = percentage absorbency under load

$W1$  = Initial (dry) weight of the sample;

$W2$  = final (wet) weight of the sample, after immersing in saline solution for 60 min

### **2.2.11 Residue test**

This test was conducted to determine the total amount of superabsorbent material, or residue, lost from the fiber matrix after it reaches equilibrium absorption. Samples were cut into small pieces of  $2 \times 2 \text{ cm}^2$  as described in previous section. Only beaker was weighed as  $W1$ . Sample was kept immersed in known amount of distilled water and allowed to reach equilibrium absorbency along with the mechanical shaking for 24 h. Sample was then removed and beaker was placed in the oven until all water evaporates. It was then weighed ( $W2$ ) again in order to determine the amount of residue that remained. Residual percentage can be determined by:

$$Y = [(W2-W1)/W1] * 100$$

Where,

$Y$  = residual percentage

### **2.2.12 Tensile test**

Tensile test measures the force required to break a sample specimen and the extent to which the specimen stretches or elongates to that breaking point. Tensile strength was measured with Instron 5948 mechanical tester at the ambient conditions. Electrospun nanofibers mat was peeled off from the aluminum foil and cut into pieces of length 6 cm, and breadth of 2 cm with thickness of approximately 0.15 mm. Similarly, the commercial samples as selected for references were cut with same dimensions with thickness varying with the sample. The sample was then placed in between pneumatic grips and the applied extension rate was 3 mm/min. Elastic modulus was then measured and compared for all the samples.

## **2.3 Results and Discussion**

### **2.3.1 Surface morphology analysis**

Surface morphology of absorbent core of selected commercial feminine sanitary napkins was examined using SEM. A representative SEM image of these fibers for sample S1 is shown here

as Figure 2.3a. Feminine sanitary napkins are made up of cellulosic fibers which are found to be in flat-ribbon like shape with width of about 40-50  $\mu\text{m}$ .

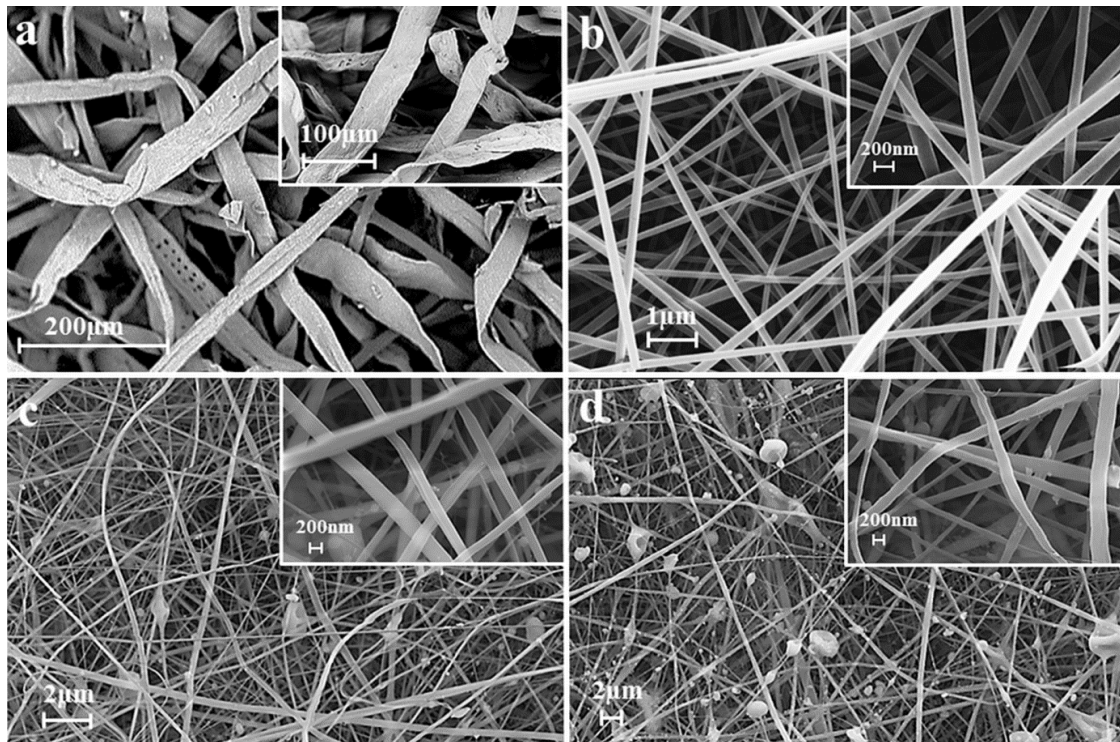


**Figure 2.3** (a) SEM image of commercial sample, S1 and FESEM images of electrospun fibers of (b) CA (c) CA5 and (d) CA10.

Electrospun CA nanofibers as shown in Figure 2.3b were long, continuous, and uniform with diameter in the range of 50-150 nm. Solution of cellulose acetate with 5 wt. % of SPA (CA5) was in suspension and its effect can be observed in the form of partially beaded fibers (Figure 2.3c). Number of beaded fibers increased on increasing the SPA concentration to 10 wt. % (CA10) as shown in figure 2.3d. However in both cases, fibers obtained were long and continuous as similar to only CA fibers. Fiber diameter for both the samples (CA5 and CA10) was measured to be in range of 50-200 nm. From FESEM image analysis, it is clearly observed that fiber diameter was reduced to more than two order of magnitude for electrospun fiber samples as synthesized in this work as compared to fabric used in commercial products.

### 2.3.2 Specific surface area

BET surface area of electrospun CA nanofibers was found to be 50.21  $\text{m}^2/\text{g}$  which decreased to 22.14  $\text{m}^2/\text{g}$  and 18.36  $\text{m}^2/\text{g}$  when SPA was added as 5 and 10 wt. % respectively. This decrease in surface area for CA-5 and CA-10 samples may be attributed mainly due to

increased fiber diameter and change in morphology from bead free to beaded fibers on encapsulation of SPA. Surface area of two commercial samples, sample S1 and S4 was measured to be 6.41 and 13.37 m<sup>2</sup>/g respectively. As we observe that surface area for electrospun CA nanofibers was significantly large compared to all other samples considered.

### 2.3.3 Free absorbency

Free absorbency test was done using distilled water, saline solution and synthetic urine respectively to test the absorption capacity of sample. Percent absorbency of electrospun cellulose acetate nanofibers with and without SPA were measured and compared with the selected commercially available feminine sanitary napkins (Figure 2.4a-c).

Figure 2.4a represents the free absorbency results in distilled water. SPA is generally added to increase the absorption capacity and is found to achieve maximum swelling in DI water. However, its encapsulation in nanofibers not only restricts its swelling but interestingly decreases the absorption capacity of CA nanofibers in DI water. For small time span of 20 sec, the percent absorbency of CA, CA5 and CA10 nanofibers was measured to be 1963.1, 1336.4 and 1446.9 % respectively. This shows that percent absorbency for pure CA nanofibers was 31.9 and 26.3 % higher than CA5 and CA10 samples respectively. In spite of increasing the time interval to 180 sec, pure CA nanofibers samples had 39.1 % and 9.5 % more absorbency as compared to CA5 and CA10 respectively. Therefore, CA nanofibers without SPA addition showed maximum percentage free absorbency. When these results were compared with commercial samples taken as reference, in DI water, it was found that the absorption capacity of CA nanofibers for time interval of 20 sec was about 48.6, 20.7, 49.2, 60.3, 61.3 and 57.1 % higher than samples S1, S2, S3, S4, S5 and S6 respectively. When time interval was increased to 180 sec, samples S1 and S2 were found to have 15.3 and 24.9 % more absorption capacity as compared to CA nanofibers respectively. However remaining four other commercial samples (S3, S4, S5 and S6) still had nearly 50% less absorbency than pure CA nanofibers.

Although specific composition of commercial samples is not known, but from physical observation sample S1 and S2 seems to have mainly superabsorbent polymers as their absorbent core however S3, S4, S5 and S6 have either no or very less SPA in the combination with some fluffy cellulosic fibers. Thus the absorption in ultra-thin products (S1 and S2) is mainly due to the superabsorbent polymers in their matrix. Therefore, absorption capacity of S1 and S2 exceeds CA nanofibers when samples were immersed in DI for longer time. On the other hand, other remaining products (S3, S4, S5 and S6) have cellulosic microfiber and

therefore their absorbency was found to be less than pure CA nanofibers primarily due to their lower surface area compared to CA nanofibers.

Figure 2.4b summarizes the absorption capacity of all nine samples in saline solution (0.9 wt. % NaCl). In saline solution also, free absorbency of CA at time interval of 20 sec was found to be 23.5 and 58.3 % higher than CA5 and CA10 respectively. When this time interval was increased to 180 sec, pure CA nanofibers still had about 57.1 and 69.1% higher absorbency than CA5 and CA10 samples. As can be seen from graph (Figure 2.4b), the absorption capacity of CA nanofibers was more than all the commercial samples over entire time interval of test. If compared at 180 sec, free absorbency of CA was measured to be 66.3, 56.1, 52.6, 56.6, 59.5 and 60.6 % more than samples S1, S2, S3, S4, S5 and S6 respectively.

Similar trend was observed for free absorbency in synthetic urine (Figure 2.4c). Absorption capacity of pure CA nanofibers for 180 s was 2333.1 % which was 35.4 and 32.2% higher than CA5 (1506.7 %) and CA10 (1582.1 %) respectively. Similarly, pure CA nanofibers were found to have 62, 51.8, 55.6, 65.9, 54.1 and 27.9 % more absorbency than S1, S2, S3, S4, S5 and S6 commercial samples respectively at the time interval of 180 s.

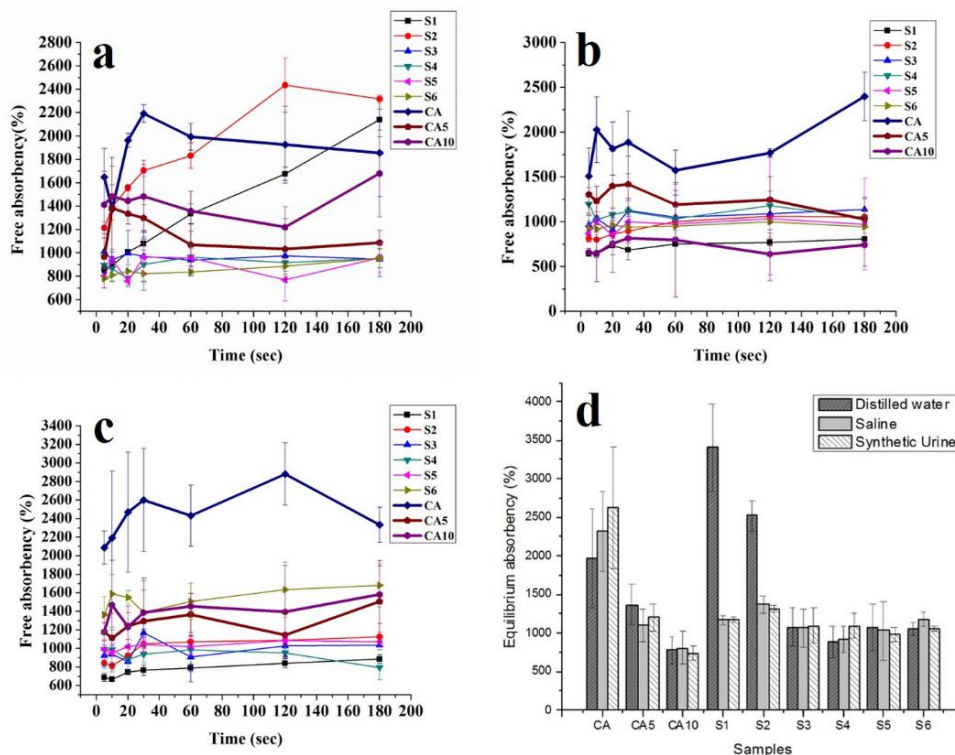


**Figure 2.4** Free absorbency test in (a) distilled water (b) saline solution (c) synthetic urine and (d) equilibrium absorbency for all samples (electrospun nanofibers CA, CA5 and CA10 and all six commercial samples).

Therefore, it is very clear that in saline solution and synthetic urine, the absorption capacity of electrospun CA nanofibers was significantly higher than any of the commercial products and also to CA5 and CA10 nanofiber samples (Figure 2.4b - c). In case of DI water also, CA nanofibers showed large absorption capacity as compared to all samples except two commercial samples S1 and S2, which were primarily based on only SAP.

#### **2.3.4 Equilibrium absorbency**

Free absorbency test was extended for time interval of 24 h in all three solutions, i.e., distilled water, saline solution and synthetic urine, to find the maximum absorption capacity, also defined as equilibrium absorbency. Figure 2.4d illustrates the percentage equilibrium absorbency of electrospun samples and selected commercial samples as references. As observed, equilibrium absorbency of pure CA nanofibers was 30.7 and 60.6 % more than CA5 and CA10 samples in DI water. Similarly, it was 52.5 and 65.4 % higher in saline solution and 54.1 and 72.1 % more in synthetic urine respectively for CA nanofibers as compared to CA5 and CA10 respectively. Therefore, it was observed that absorption capacity for CA nanofibers encapsulated with SPA (CA5 and CA10) was less even after allowed to swell for 24 h in all three solutions.

Furthermore while comparing the equilibrium absorbency in DI water with commercial samples, we found that absorbency of S1 and S2 was 73.3 and 28.2 % higher than CA samples. This is again because of the swelling of superabsorbent polymers present in these ultra-thin products (S1 and S2) on increasing the time for immersion in DI water. However for other commercial samples (S3, S4, S5 and S6), equilibrium absorbency in DI water was 45.3, 55.1, 45.6 and 46.45 % less than pure CA nanofibers samples owing to their reduced surface area. Interestingly, the equilibrium absorbency of S1 decreases to about 65.7 and 65.5% in saline solution and synthetic urine respectively while comparing it in DI water. Similarly for S2 commercial sample, there is a decrease of 45.7 and 47.8 % in saline solution and synthetic urine respectively as compared to absorbency in DI water. This behavior can be explained as follows: SPA at molecular structure contains sodium carboxylate groups on the main chain. Sodium gets detached from the chain, leaving only carboxyl ions, when it comes in contact with water.<sup>2</sup> This allows the sodium ions to move freely within the network, which contributes to the osmotic pressure within the gel. The mobile positive sodium ions however cannot leave the gel because they are still weakly attracted to the negative carboxylate ions along the polymer. So the driving force for swelling is the difference between the osmotic pressure inside and outside the gel. Increasing the level of sodium outside of the gel will lower the osmotic pressure and



reduce the swelling capacity of the gel.<sup>16</sup> This swelling mechanism of SPA explains the sudden decrease in the equilibrium absorbency of commercial sanitary napkins (S1 and S2) in both saline solution and synthetic urine.

From the free absorbency and equilibrium absorbency results it can be concluded that the electrospun CA nanofibers have significantly large absorption capacity for saline solution and synthetic urine as compared to the commercial products in all the categories of use. Also, the encapsulation of SPA in these CA nanofibers (CA5 and CA10) is decreasing the absorption capacity of nanofibers even when allowed to swell freely for 24 h. Therefore, it is very clear that use of SPA in CA nanofibers does not facilitate in enhancing the absorption efficiency of the matrix.

### 2.3.5 Absorbency under load (AUL)

This test measures the effect of mechanical compression on the swelling process of sample and is an important consideration for the proposed use of CA nanofibers for female hygiene applications. The compressive load applied on the sample changes the shape of the sample and may alter the surface properties like suppressing the internal structure. As a result, there is decrease in the absorbency under load compared to the free swelling i.e., equilibrium absorbency in saline solution as shown in figure 2.5.

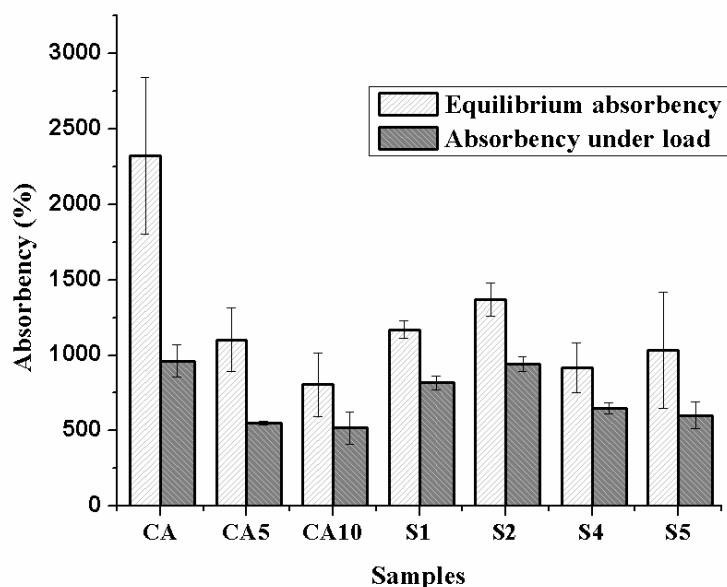


**Figure 2.5** Absorbency under load in saline solution for electrospun nanofibers samples and commercial samples (S1, S2, S3 and S4).

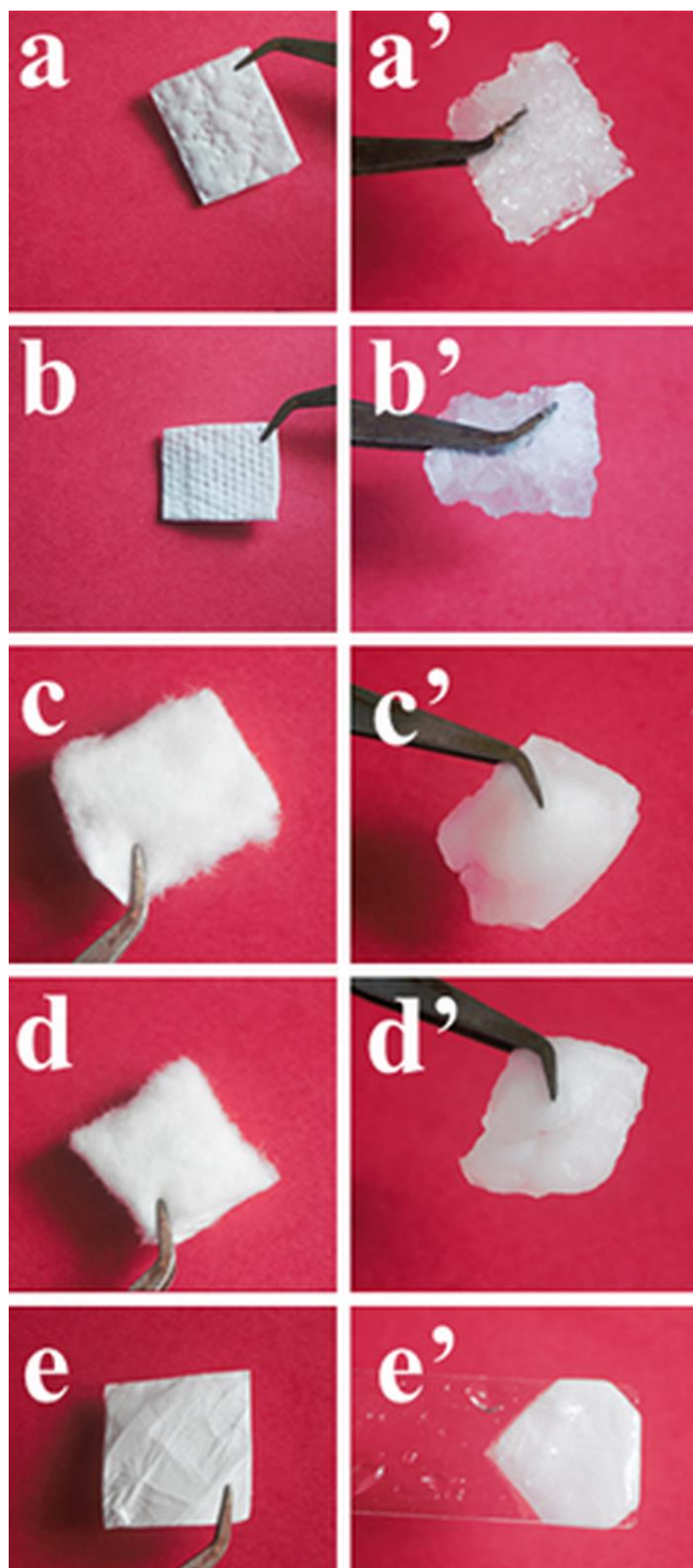
Absorbency under load for electrospun CA nanofibers was measured to be 961.9 % which was reduced to 550.1 and 517.7 % for CA5 and CA10 respectively. This means that CA nanofibers have 42.8 and 46.2 % more absorbency under load than CA5 and CA10 respectively. Similarly absorbency under load for pure CA nanofiber was found to be 15.1, 2.2, 32.8 and 37.5 % more than S1, S2, S4 and S5 samples respectively. These results also confirm that CA nanofibers exhibited much improved performance as compared to any other samples including all commercial samples.

### **2.3.6 Residue test**

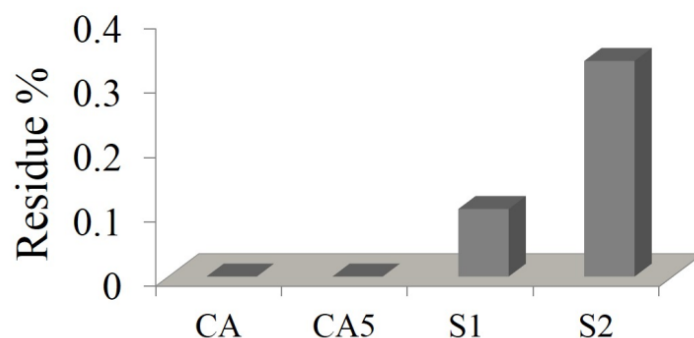
The amount of losses from the matrix was quantified by using residue test. The cellulosic fibers or loosely held SAP granules in commercial samples mainly contribute towards the residue from absorbent core.

Figure 2.6 represents the structure of absorbent core of commercial samples and CA nanofibers before (figure 2.6a-e) and after dipping in distilled water (figure 2.6a'-e') for 10 minutes. SAP granules swell upon absorbing liquid and form a liquid impermeable wall of gel and inhibit further movement of liquid. Therefore, these polymers are randomly distributed within the absorbent core.<sup>2</sup> Smaller SAP granules increase the absorption rate because of increase in the surface area, but they have tendency to fall out of the matrix, therefore contributing towards the residue as shown in figure 2.6a'-b'. Whereas in some other cases, loosely held cellulosic fibers in the absorbent core contribute to the residue (figure 2.6c'-d'). However importantly there is no major structural change in CA nanofibers except little shrinkage (figure 2.6e') as compared to commercial samples.

Quantitative results of residue tests are summarized in figure 2.7. Electrospun nanofibers of pure CA and with SPA (CA5) have almost negligible residue compared to the feminine sanitary napkins, S1 (0.11 %) and S2 (0.34%) respectively. For other commercial samples S3, S4, S5 and S6, whole cellulosic fiber matrix disintegrates due to mechanical shaking for 24 h done along with equilibrium absorbency. Therefore entire initial weight of samples acts as residue and thus not compared in figure 2.7. The electrospun CA nanofibers are strongly entangled and therefore does not contribute to any residue. Same was true after encapsulating with SAP (CA5 and CA10).



**Figure 2.6** Pictorial representation of the absorbent cores of commercial samples (a) S1 (b) S2 (c) S5 (d) S4 and electrospun CA nanofibers (e). Figure a'-e' shows the changes after dipping in distilled water for 10 minutes in respective samples.



**Figure 2.7** Residue test for electrospun fiber samples (CA and CA5) and commercial samples (S1 and S2).

### 2.3.7 Tensile test

The inadequate tensile strength of absorbent core may lead to its breakage or tearing which may result in the leakage of fluid thereby decreasing the product's efficiency. Therefore, mechanical properties of electrospun CA nanofibers were measured and compared with other commercial samples. These results are represented in figure 2.8.

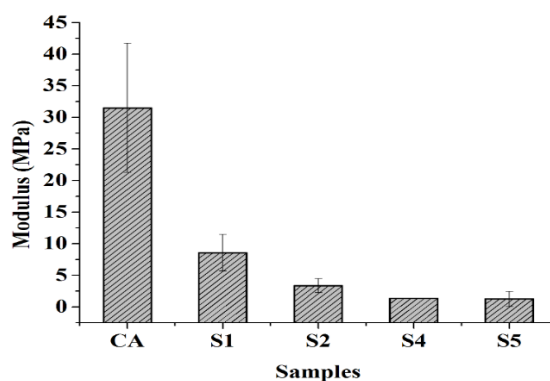


**Figure 2.8** Young's Modulus for different samples (electrospun CA nanofibers and commercial samples S1, S2, S4 and S5).

There is a significant difference between the elastic modulus of electrospun CA nanofibers and commercial samples. The absorbent core of commercial samples (S1, S2, S4 and S5) is mainly made by loosely held cellulosic fibers and strength is provided by using different layers, above and below the core. However in case of CA nanofibers, due to compact structure and entanglement of nanofibers, modulus of elasticity was found to be  $31.5 \pm 10.2$  MPa. For S1, S2, S4 and S5, the modulus are  $8.6 \pm 2.9$ ,  $3.4 \pm 1.1$ ,  $1.4 \pm 0.1$  and  $1.3 \pm 1.2$  MPa respectively (Figure 8). These results show that mechanical strength of pure CA nanofibers was more than

any other commercially available samples and thus directly can be used as absorbent core in female hygiene products.

## **2.4 Conclusions**

We have fabricated CA electrospun nanofibers with and without encapsulating different amount of SPA into their fiber matrix and successfully demonstrated their application in female hygiene products. Free absorbency, equilibrium absorbency and absorbency under load were carried out in three different mediums (DI water, saline solution and synthetic urine) for all samples fabricated in this work and results were compared further with a wide variety of commercially available female sanitary napkins used for various stages during female menstrual cycles. In case of DI water, CA nanofibers performed significantly better than two other nanofibers samples encapsulated with SPA and also outperformed most of these commercial samples used for reference. Only in case of free absorbency and equilibrium absorbency in DI water, two commercial samples (S1 and S4) which were primarily based on SAP only, showed more absorbency than CA electrospun nanofibers. However more importantly, only CA electrospun nanofibers showed significantly large absorbency in all conditions as compared to any other fabricated as well as commercial samples in saline solution and synthetic urine solutions.

Equally important, residual percentage for all electrospun nanofiber samples (CA, CA5 and CA10) was found to be negligible. Furthermore, tensile strength was also found to be more for electrospun CA nanofibers as compared to SPA encapsulated nanofibers and commercial samples.

Most importantly, we found that loading of SPA in CA nanofibers not only decreased the surface area but also restricted SPA to swell resulting in decreased absorption capacity than only CA nanofibers. This clearly suggest that use of SPA (or in general SAPs) can be eliminated if CA nanofibers are used to make the absorbent core in feminine sanitary napkins without compromising with the absorption efficiency. This will not only reduce the health related risks such as toxic shock syndrome linked with the use of SAPs but also make the disposable female sanitary napkin products more environment friendly, as SAPs are generally non-biodegradable.

## **2.5 Acknowledgements**

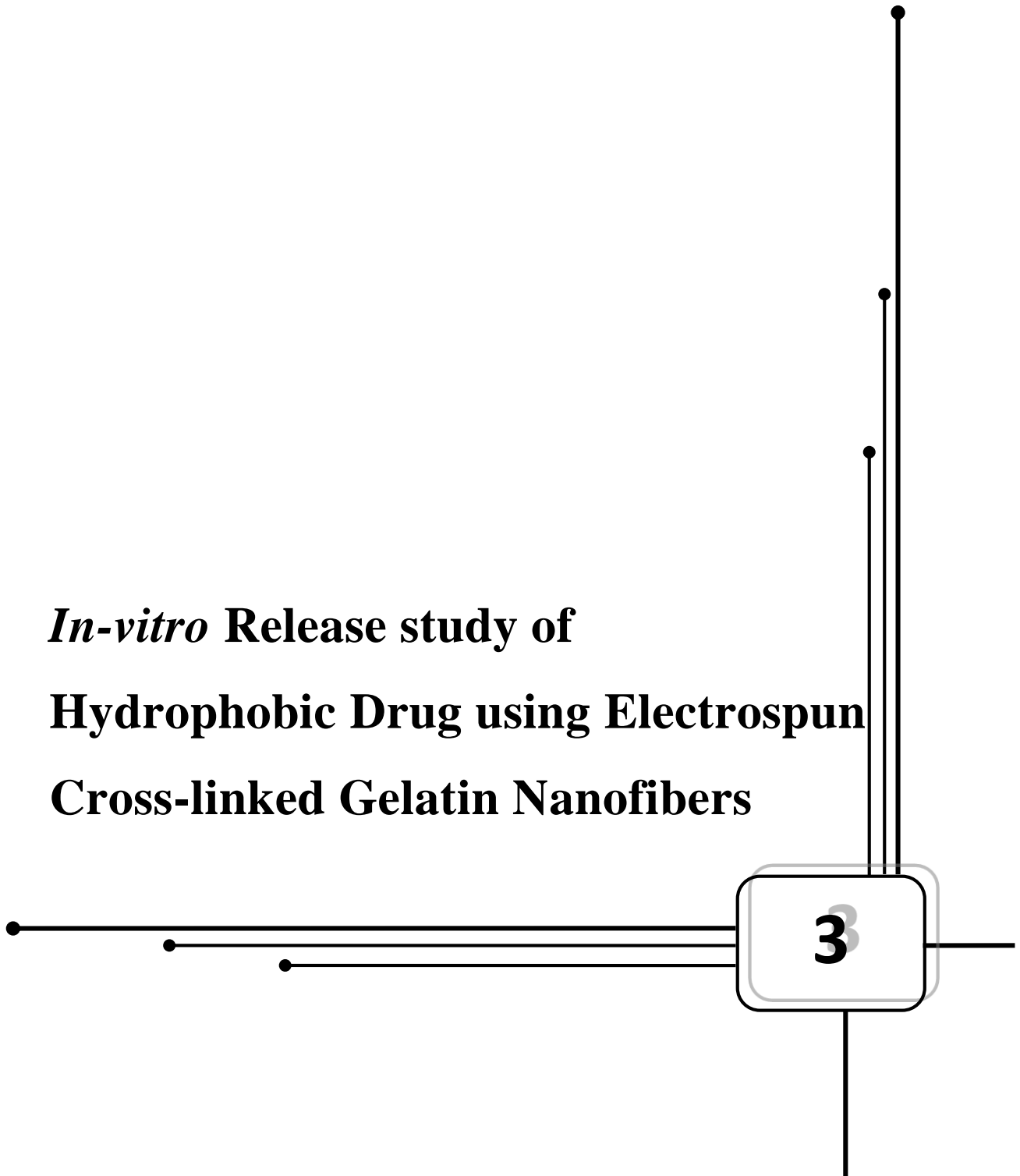
We would like to express our thanks to Anand Kumar for his help in FESEM imaging and BET measurements.

## References

1. Garg, R.; Goyal, S.; Gupta, S. India Moves Towards Menstrual Hygiene: Subsidized Sanitary Napkins for Rural Adolescent Girls-Issues and Challenges. *Maternal and Child Health Journal*, 16 (2012), 767-774.
2. Das, D. In *Composite Nonwoven Materials*; Das, D., Pourdeyhimi, B., Eds.; Woodhead Publishing: United Kingdom, 2014; p 74.
3. Mohammad, J. Z.; Kourosh, K. Superabsorbent Polymer Materials: A Review. *Iranian Polymer Journal*, 17 (2008), 451-477
4. Kumar, K.S. Is Your Sanitary Napkin Safe, *The New Indian Express*, August 28, 2013, Website.<http://www.newindianexpress.com/cities/bangalore/Is-your-sanitary-napkin-safe/2013/08/28/article1755252.ece>
5. Berkley, S. F.; Hightower, A. W.; Broome, C. V.; Reingold, A. L. The Relationship of Tampon Characteristics to Menstrual Toxic Shock Syndrome. *The Journal of the American Medical Association*, 258 (1987), 917-920.
6. Ramakrishna, S.; Fujihara, K.; Eong, T.W., Lim, T.; Ma, Z. *An Introduction to Electrospinning and Nanofibers*. World Scientific Publishing Co. Pte. Ltd.: Singapore, 2005.
7. Cramariuc, B.; Cramariuc, R.; Scarlet,R.; Manea, L. R.; Lupu, I. G.; Cramariuc, O. Fiber Diameter in Electrospinning Process. *Journal of Electrostatics*, 71 (2013), 189-198.
8. Formhals, A. Process and Apparatus for Preparing Artificial Threads. US. Patent 1,975,504, October 2, 1934.
9. Doshi, J.; Reneker, D.H. Electrospinning Process and Applications of Electrospun Fibers. *Journal of Electrostatics*, 35 (1995), 151-160.
10. Huang, Z-M.; Zhang, Y-Z.; Kotaki, M.; Ramakrishna, S. A Review on Polymer Nanofibers by Electrospinning and Their Applications in Nanocomposites. *Composites Science and Technology*,63 (2003), 2223-2253.
11. Frey, M.W. Electrospinning Cellulose and Cellulose Derivatives. *Polymer Reviews*, 48 (2008), 378-391.
12. Hubbe, M. A.; Ayoub, A.; Daystar, J. S.; Venditti, R. A.; Pawlak, J. J. Enhanced Absorbent Products Incorporating Cellulose and Its Derivatives: A Review. *BioResources*, 8 (2013), 6556-6629.

13. Konwarh, R.; Karak, N.; Misra, M. Electrospun Cellulose Acetate Nanofibers: The Present Status and Gamut of Biotechnological Applications. *Biotechnology Advances*, 31 (2013), 421-437.
14. Zhou, W.; He, J.; Cui, S.; Gao, W. Studies of Electrospun Cellulose Acetate Nanofibrous Membranes. *The Open Materials Science Journal*, 5 (2011), 51-55.
15. Frazier, M. Superabsorbent Nanofiber Matrices. Ph.D. Thesis, The University of Akron, OH, USA, 2006.
16. Elliott, M. Superabsorbent Polymers; BASF Aktiengesellschaft: Ludwigshafen Germany, 2004.

***In-vitro* Release study of  
Hydrophobic Drug using Electrospun  
Cross-linked Gelatin Nanofibers**





## **Abstract**

We report the synthesis of gelatin nanofibers by electrospinning, followed by testing them as a potential drug carrier for oral drug delivery system. Piperine is used as a model hydrophobic drug. Electrospun gelatin nanofibers were crosslinked by exposing to saturated glutaraldehyde (GTA) vapors, to improve their water resistive properties. An exposure of 6 min was adequate to maintain the morphology of nanofibers, tested by soaking in different pH solutions for 24 h at room temperature. Scanning electron microscopy (SEM) imaging, Fourier transform infrared (FTIR) spectroscopy and thermogravimetric analysis (TGA) were done to study physiochemical properties of nanofibers, stability of drug and effect of crosslinking. The pH of release medium was varied as per the gastrointestinal (GI) tract for in vitro drug release study. The amount of drug release decreases with increase in crosslinking degree and increases in higher pH. Results illustrate good compatibility of hydrophobic drug in gelatin nanofibers and further demonstrates the controlled drug release by varying crosslinking time and pH of release medium.

### 3.1 Introduction

Controlled drug delivery prevents over-dosing of drug and thus reduces the toxic effects associated with it. Efficacy of administered drug can be maintained by keeping the drug concentration in the body within its therapeutic window<sup>1</sup>. Due to the convenience of delivery and better patient compliance, oral route is mostly preferred<sup>2</sup>. To administer the drug release in the oral route, drug molecule is generally encapsulated in excipients, which protects the bioactive molecule from enzymatic degradation in gastrointestinal (GI) tract. These excipients can be in various physical forms such as nanoparticles<sup>3</sup>, hydrogels<sup>4-5</sup>, thin films<sup>6-7</sup>, micelle<sup>8-9</sup>, micro/nanogels<sup>10-11</sup> etc. However over the past decade, nanofibers have been demonstrated as a potential drug delivery systems due to their large surface area to volume ratio and controllable porosity, thereby resulting high drug loading capacity<sup>12</sup>. Among the several techniques to fabricate nanofibers such as phase separation, self-assembly, electrospinning etc.; electrospinning is mostly preferred due to its versatility in terms of use of large number of polymers, ease of control on fiber size with well-defined morphology and better scalability<sup>12-14</sup>.

Gelatin is one of the most commonly used FDA approved biopolymer, as an excipient because of its biocompatibility, biodegradability, muco-adhesiveness and easy availability. It has generally been used as drug carrier in different forms such as hydrogels, microspheres, nanoparticles etc.<sup>15</sup> Although electrospun gelatin nanofibers have been reported in recent past for biomedical applications including tissue engineering, scaffold/ bone repair, wound healing and drug delivery but all these studies use gelatin based electrospun composite fibers.<sup>16-20</sup> To the best of our knowledge, this is first effort not only to explore the potential of pure gelatin based electrospun nanofibers as a carrier but also for a hydrophobic drug.

Electrospun gelatin nanofibers are water soluble, which limits its application and long term use<sup>21</sup>. The crosslinking agent like formaldehyde<sup>22</sup>, genipin<sup>23</sup>, glutaraldehyde (GTA) etc.<sup>24</sup> have been reported in the literature, to modify gelatin via its amino, carboxyl or hydroxyl group respectively. GTA is most widely used because of its efficiency in stabilising collagenous materials<sup>21</sup>, reducing biodegradation of material. Also, it is easily available, has low cost and can accomplish excellent crosslinking in a relatively short time period.

The objective of present work is to study the stability and release of hydrophobic drug from electrospun hydrophilic carrier. Piperine is selected as model hydrophobic drug. Piperine (1-piperoyl piperidine) is commonly known for its bio-enhancing effect on

other co-administered drug<sup>25</sup>. It has been reported that piperine increases the bio-availability of curcumin, an anti-cancerous drug by 2000% in humans<sup>26</sup>. It also shows anti-depression, anti-inflammatory, anti-bacterial properties<sup>25</sup>.

Gelatin nanofibers were prepared using electrospinning and cross-linked using saturated GTA vapours. Further, in-vitro release studies were performed at varying pH conditions matching human GI tract environment. This article, co-relates the morphology, degradation study, stability of hydrophobic drug and effect of crosslinking with in vitro release study of hydrophobic drug through gelatin nanofiber.

## **3.2 Experimental methods**

### **3.2.1 Materials**

Gelatin (Type A, 175 bloom), Piperine (98%), Hydrochloric acid (ACS,36.5-38.0%), Gluteraldehyde (25% v/v aqueous solution), Acetic acid (glacial, ACS, 99.7+%), Sodium hydroxide pallets (98%), phosphate buffer saline (pH 7.4) were purchased from Alfa Aesar. Deionized water (DI) (Milli Q, resistivity 18.1 MΩ.cm) were used throughout the experiments. All the chemicals were used without further purification.

### **3.2.2 Preparation of electrospinning solution**

Gelatin (Type A) was dissolved in acetic acid solution (20%, v/v in distilled water) at 20% (w/v). The solution was stirred on a magnetic stirrer for 3 h at room temperature to get clear and homogenous solution, which was used to prepare gelatin nanofibers (GNF). In the prepared gelatin solution, piperine (2 mg/ml) was added and stirred for 2 h, to prepare piperine loaded gelatin nanofibers (G-P NF).

### **3.2.3 Electrospinning**

Electrospun nanofiber were prepared using electrospinning apparatus (E Spin Nanotech Pvt. Ltd, India). The spinning solution was transferred to 3 mL syringe with needle diameter of 21 gauge, by carefully avoiding air bubbles. The electric potential of 12 kV was applied between tip and collector, kept at a distance of 10 cm. The solution feed rate was 5 µl/min. Electrospinning process was carried out at room temperature and aluminium foil was used as a substrate for deposition

### **3.2.3 Crosslinking electrospun membranes**

Electrospun GNF and G-P NF membranes are soluble in water, therefore, crosslinking was done by exposing it to saturated vapor of GTA (25% v/v aqueous solution). Both GNF and G-P NF, with and without substrate (i.e., aluminium foil), were cut into 2X2 cm<sup>2</sup> sample sizes. These samples were placed inside the glass desiccator having 20 ml of GTA solution and was then closed. Exposure to GTA vapour was done at room temperature for different time intervals i.e, 2, 4, 6, 8 and 10 min respectively.

### **3.2.4 Surface morphology**

The morphology of the GNF and G-P NF, with and without crosslinking were examined by field emission scanning electron microscopy (FESEM) (Carl Zeiss, SUPRA 40). The samples were sputter-coated with gold, to reduce charging effect.

### **3.2.4 Specific Surface Area (SSA) measurement**

The Brunauer–Emmett–Teller (BET) surface area of non-crosslinked electrospun GNF and crosslinked for 6 min (GNF 6) with GTA vapor was determined by N<sub>2</sub> physisorption using Micromeritics ASAP 2020 physisorption analyzer. The sample mass was about 100mg. All samples were degassed at room temperature for 6 h in nitrogen. The SSAs were determined by a multi-point BET measurement with nitrogen as the adsorbate.

### **3.2.5 FTIR Spectroscopy**

Electrospun non-crosslinked and crosslinked GNF and G-P NF were characterized by using Fourier transform infrared (FTIR) spectrometer (Bruker Alpha-P) in 500-4000 cm<sup>-1</sup> range

### **3.2.6 Thermogravimetric analysis**

Thermogravimetric analysis (TGA) of G-P NF membrane and 6 min cross-linked samples was carried out using platinum pan in helium atmosphere (pyris 1, Thermogravimetric analyser, Perkin Elmer). Sample weight varies from 5 to 10 mg and samples were heated from room temperature to 800 °C at a heating rate of 10 °C/min.

### **3.2.7 Release medium**

To study the prepared samples for application in oral drug delivery system, pH of release medium was varied as per the gastrointestinal tract (GI) in human body. The upper

portion of stomach have pH 4-6.5, which decreases to pH 1.5-4 in lower portion due to gastric acids. The pH of small intestine (duodenum) varies from pH 7-8, where maximum absorption of nutrients takes place. Therefore, pH 1.2, pH 6, pH 7.4 and pH 8 are selected for further study.

### **3.2.8 Degradation study**

Degradation study helps in determining the stability of the cross-linked electrospun mat in different physiological pH solutions. For degradation study, 5×5 cm<sup>2</sup> of electrospun GNF and G-P NF, cross-linked over different time intervals, were kept in 25 ml solutions of pH 1.2, pH 6, and pH 7.4 and pH 8 respectively in mechanical shaker (Remi RIS-24 plus) for 24 h, at 37<sup>0</sup> C and 150 RPM.

### **3.2.9 In-vitro release study**

The release of drug i.e., piperine from electrospun nanofiber mats was measured by placing 5×5 cm<sup>2</sup> of drug loaded fiber mat in 10 ml of release medium at different physiological pH levels (1.2, 6, 7.4 and 8). The temperature and stirring of the system were maintained at 37°C and at 50 RPM, respectively, to mimic the physiological conditions. An aliquot sample was withdrawn, at fixed time intervals for the analysis and same amount of fresh solution was added back to the release medium to maintain the sink condition. After centrifuging (Wise Spin, CF-10) the sample for 2 min at 1300 RPM, the samples were analysed using an UV spectrophotometer (Perkin Elmer Lambda 35) at 342nm as λ<sub>max</sub> for Piperine. The results were presented in terms of cumulative release as a function of time:

$$\text{Cumulative amount of release (\%)} = (C_t / C_\infty) * 100$$

Where, C<sub>t</sub> is the amount of piperine released at time t and C<sub>∞</sub> refers to total amount of drug loaded in 5x5 cm<sup>2</sup> sample.

All results were presented as mean ± standard deviation (SD) of three independent experiments to confirm reproducibility of the findings.

### 3.3 Results and discussion

#### 3.3.1 In-vitro bio-degradation of the mat

Figure 3.1(a) shows the effect of crosslinking on GNF. Lysine is one of the amino acids present in gelatin, which is responsible for crosslinking with aldehyde group of GTA. The crosslinking mechanism is described in the study of Farris et.al.<sup>24</sup> After crosslinking, sample became light yellowish and shrinks. Therefore, membranes are not peeled from aluminium foil before crosslinking with GTA vapour, in order to avoid excessive shrinkage of membrane on cross linking.

Degradation study was done with the aim to check the stability of samples up to 24 hr. Cross-linked samples over different time intervals (non-cross-linked i.e., 0 min and cross-linked for 2, 4, 6, 8 and 10 min) were undergone the degradation at different pH (1.2, 6, 7.4 and 8) solutions.

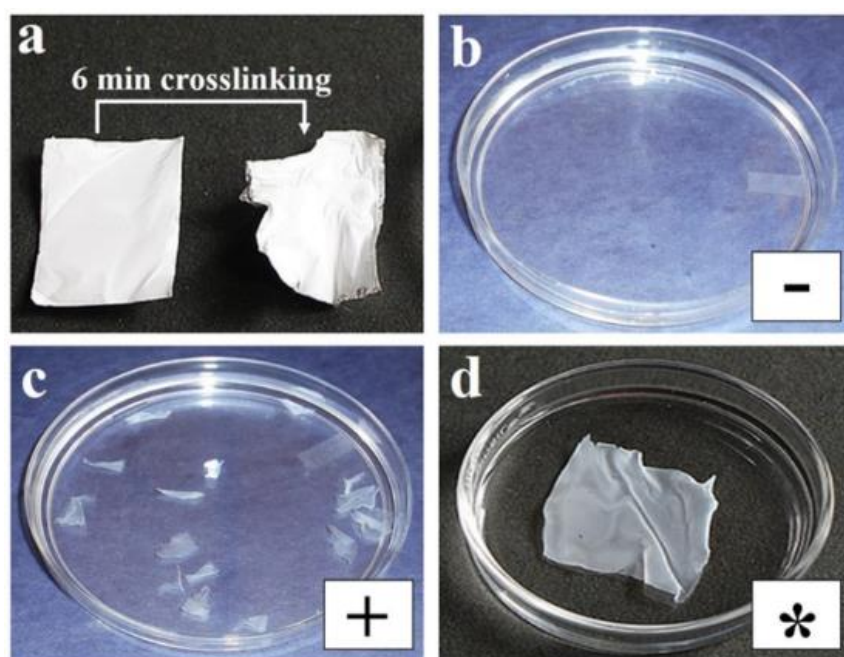


**Figure 3.1** Digital images representing, (a) effect of crosslinking for 6 min on GNF (b) completely degraded (c) partially degraded and (d) intact membrane.

Results of degradation study for electrospun GNF and G-PNF membrane are summarized in Table 1. Fig. 1 (b)-(d) represents the morphology of membrane represented by symbols in Table 1. It can be seen that, the non-cross-linked samples dissolve immediately because of hydrophilic nature of gelatin. The samples crosslinked

for 2 and 4 min degrades in acidic medium within 24 hrs, therefore are not suitable for this study. Samples cross-linked for 6 min or above were found to be stable even after 24 h in all pH conditions. Therefore, 6 min crosslinking time was selected for further analysis.

**Table 3.1** Summary of degradation study for GNF and G-P NF crosslinked over different time interval, in dissolution medium of different pH

pH of dissolution medium	Time of crosslinking with GTA (25% v/v) vapour											
	GNF						G-P NF					
	0	2	4	6	8	10	0	2	4	6	8	10
1.2	-	+	+	+	*	*	-	+	+	*	*	*
6	-	+	*	*	*	*	-	+	*	*	*	*
7.4	-	*	*	*	*	*	-	+	*	*	*	*
8	-	*	*	*	*	*	-	*	*	*	*	*

Where, ‘-’ means completely degraded, ‘\*’ means not degraded and ‘+’ refers to partial degradation in the dissolution medium after soaking for 24 h.

### 3.3.2 Surface morphology

The surface morphology of electrospun GNF and G-P NF membrane with and without crosslinking are represented in figure 3.2. SEM micrographs shows continuous, long nanofibers with fiber diameter in the range of 50-200 nm for both GNF and G-P NF as shown in figure 3.2.a and 3.2.c respectively.

Due to the hydrophilic nature of gelatin, it allows the water molecules along with GTA molecules from the saturated vapour, leading to changes in morphology on crosslinking even for only 6 min. It can be observed that the fibers fuse with one another at contact points (figure 3.2.b), as a result of the partial dissolution of the fiber segments when they come in contact with moisture rich GTA vapour<sup>21-27</sup>. However, in case of G-P NF, presence of hydrophobic piperine discourages the interaction of water molecules in GTA vapour with fibers. It leads to relatively less fusing in fibers at the point of contact of fibers, though the time of crosslinking is same (figure 3.2.d). Also, there are no physical changes on the morphology due to presence of piperine in GNF, showing successful loading of hydrophobic piperine in hydrophilic GNF membrane.

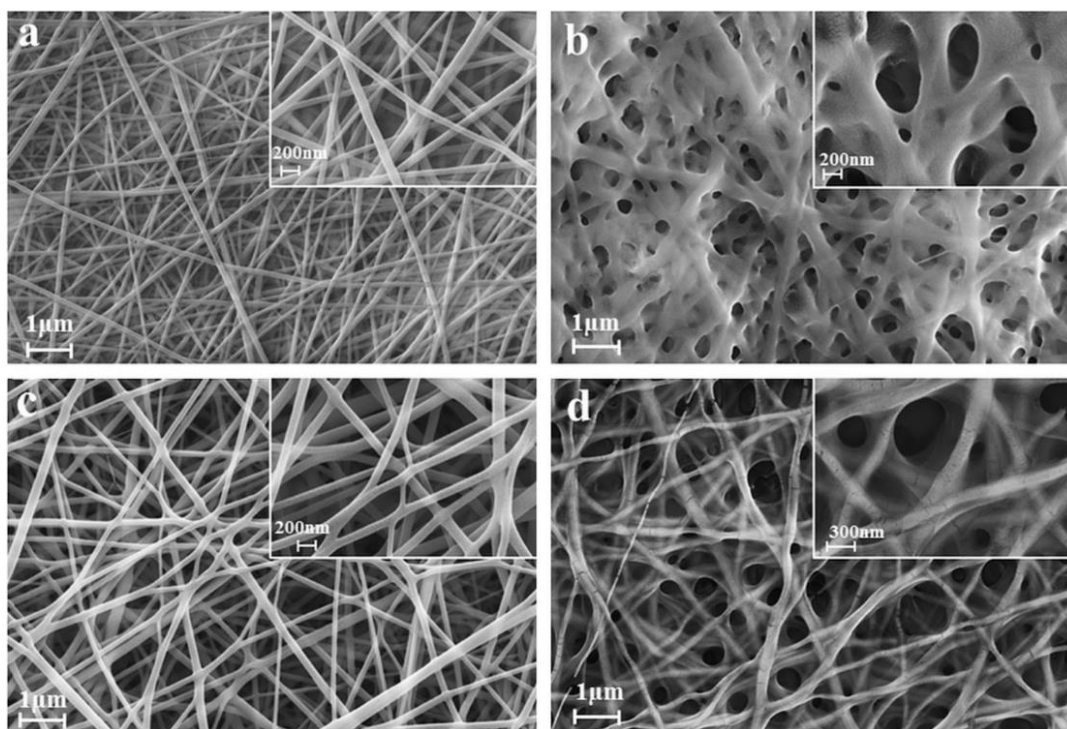


**Figure 3.2** FESEM images of (a) as-spun GNF, (b) GNF after crosslinking with GTA vapor for 6 min, (c) as-spun G-P NF, and (d) G-P NF after crosslinking with GTA vapor for 6 min.

### 3.3.3 Specific surface area

BET surface area of electrospun GNF was found to be  $23.4 \text{ m}^2/\text{g}$ . On exposing for 6 min with saturated GTA vapor, the BET surface area decreased to  $18.2 \text{ m}^2/\text{g}$ . A similar increase in total pore volume was also observed ( $0.063$  and  $0.05 \text{ cm}^3/\text{g}$  for as-spun and 6 min cross linked GNF). However average pore diameter as measured by BJH method remains almost unchanged to  $10.8$  and  $10.9 \text{ nm}$  for as-spun and 6 min cross linked fiber samples respectively. This decrease in surface area and total pore volume can be explained due to fusing of fibers on coming in contact with water molecules present along with GTA molecules, as illustrated in SEM analysis. Therefore, the electrospun GNF membrane fabricated as carrier for loading drug has sufficiently large surface area, even after crosslinking with GTA vapor.

### 3.3.4 FTIR analysis

To know the chemical composition, effects of crosslinking and the interactions between the drug and polymer matrix FTIR/ATR analysis were attempted. The absorption bands



at  $3273.10\text{ cm}^{-1}$  (N-H stretch),  $1631.66\text{ cm}^{-1}$  (amide I, C=O and C-N stretch),  $1536.31\text{ cm}^{-1}$  (amide II, N-H bend and C-H stretch) and  $1237.88\text{ cm}^{-1}$  (amide III) are the characteristic bands of GNF (figure 3.3.a) <sup>27</sup>. On crosslinking, aldehyde group (-CHO) of GTA reacts with the amino group of the lysine which is present in gelatin and amino (-NH<sub>2</sub>) groups interact with the carbonyl groups of GTA to form new covalent (-C=N-) bonds<sup>24</sup>. During crosslinking,  $3273.10\text{ cm}^{-1}$  (N-H stretch) peak shows minor increase to  $3275.60\text{ cm}^{-1}$  on crosslinking for 6 min because of hydrogen bond formation between amino group of gelatin and carbonyl group of GTA. Similarly, first amide I (C=O and C-N stretching) peak shifts from  $1631.66\text{ cm}^{-1}$  to  $1637.80\text{ cm}^{-1}$  indicating its interaction during crosslinking. Similar trends are also observed in amide II and III peaks of gelatin, which confirm the hydrogen bonding with aldehyde groups of GTA.

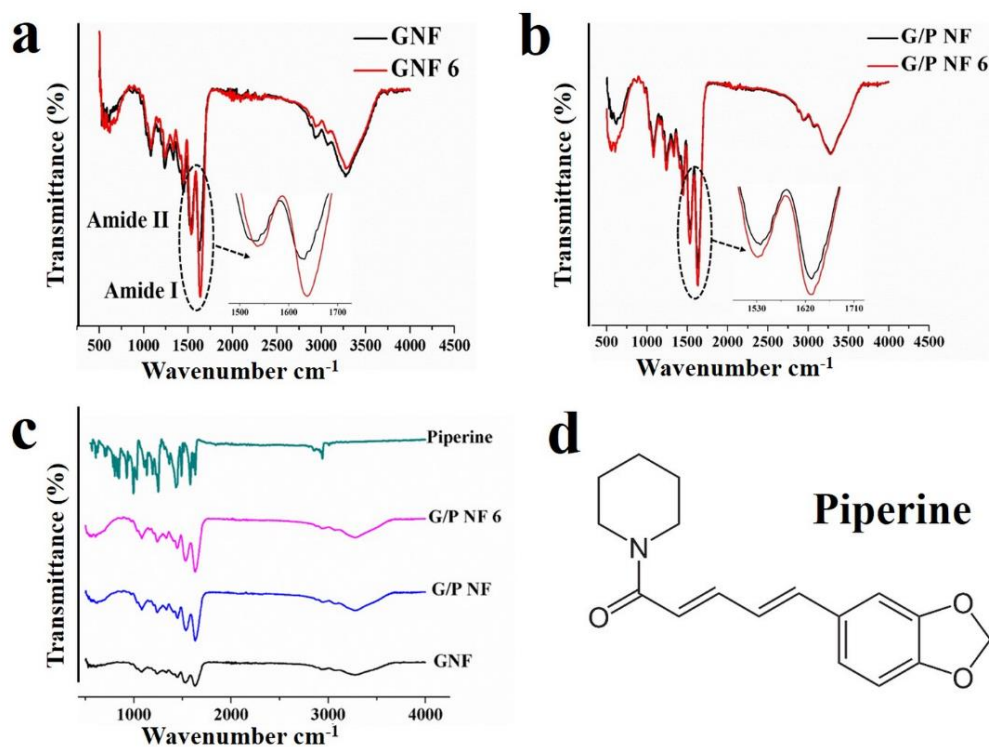


**Figure 3.3** Effect of crosslinking on (a) GNF and (b) G-P NF ; (c) stability of piperine (d) chemical structure of piperine used as a drug.

Figure 3.3.b represents the effect of crosslinking in presence of piperine. As can be seen there is no difference in the characteristic peaks on crosslinking. It can be explained by the presence of hydrophobic piperine, which discourages water-GTA vapor molecules

to crosslink gelatin. This phenomenon leads to less degradation of piperine loaded sample as discussed in morphology study in figure 3.2.d.

The characteristic peaks of functional groups of piperine are not visible in G-P NF membrane as in figure 3.3.c. Also, there are no new peaks on piperine loading in GNF and crosslinking with GTA vapor, indicating no physical or chemical interaction between hydrophobic piperine drug and hydrophilic gelatin excipient. Therefore, one can conclude that piperine was successfully loaded and was found to be stable in both GNF and crosslinked G-PNF samples.

### 3.3.5 Thermal properties

TGA analysis of as-spun GNF and 6 min crosslinked GNF membrane are shown in figure 3.4. Initial weight loss of 6.6% and 7.5% for as-spun and crosslinked GNF between 35 to 100 °C is due to the elimination of absorbed and bounded water molecules in the membrane. Second stage of weight loss, from 250 to 450 °C corresponds to thermal degradation of gelatin due to the breakage of protein chain. For as-spun GNF, this was found to be 56.3% that was reduced to 43.9% for 6 min crosslinked GNF sample. Thus, crosslinking GNF with GTA vapour, for 6 min, increased the thermal stability and residue percentage as well. Therefore, besides improving the water resistive property of GNF, GTA also increases the thermal stability of GNF membrane.

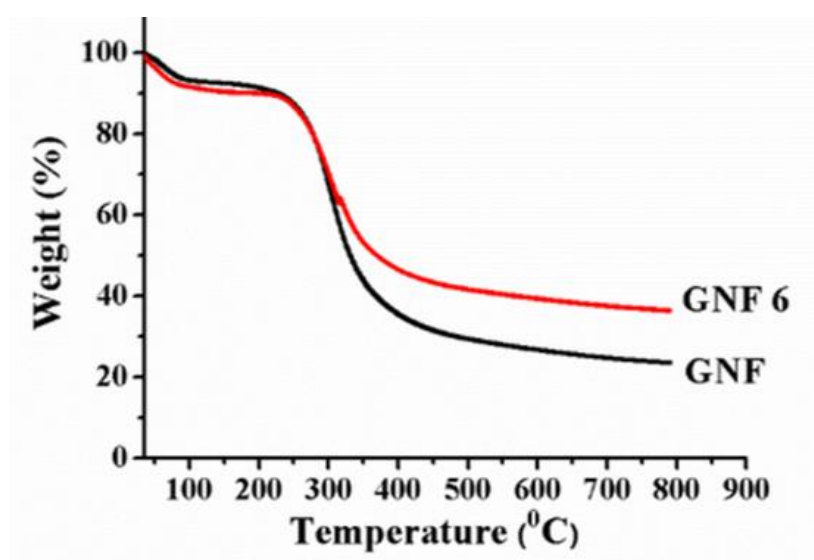


**Figure 3.4** Thermogram of as-spun and 6 min crosslinked GNF membrane

### 3.3.6 In vitro drug release study

The drug release process depends upon various factors like polymer matrix property, release medium and nature of drug molecules. The release of drug from a polymer matrix is modulated by diffusion of drug and / or degradation of the polymer matrix. Insufficient physical and chemical interactions (as evident in the FTIR study) between the hydrophobic drug molecules and the hydrophilic polymer matrix led to sudden release of drug molecules within few hours from the surface. As the G-PNF membrane swells, due to presence of water molecules, the osmotic pressure provides the driving force for release of drug in the release medium. Therefore, after 2 h, there is sustained release of drug as drug diffuses to the release medium through the carrier gradually.

#### 3.3.6.1 Effect of pH value of release medium

The various cross-linked G-PNF membranes i.e, 4 min, 6 min and 8 min, are referred as G-PNF 4, G-PNF 6 and G-PNF 8 respectively. The in vitro drug release studies were performed in different pH conditions as per the human GI tract environment i.e, pH 1.2 (lower portion of stomach), pH 6 (upper portion in stomach), pH 7.4 and pH 8 (small intestine) as shown in figure 3.5.

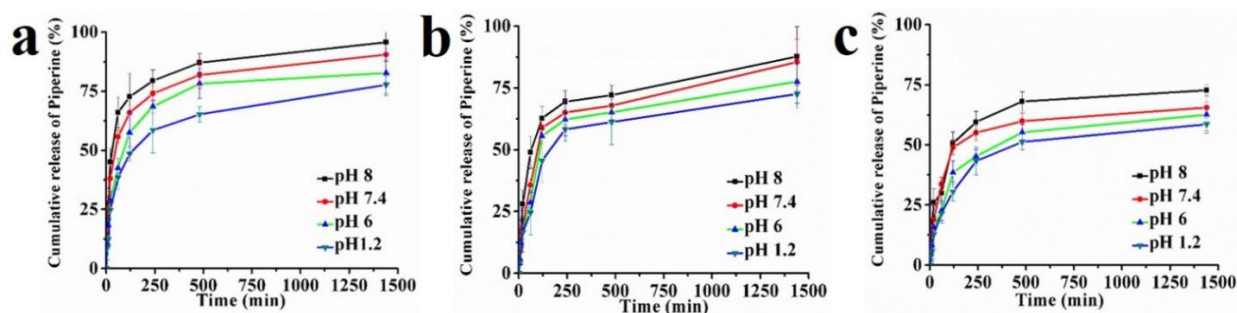


**Figure 3.5** Cumulative release of piperine for (a) 4 min (b) 6 min and (c) 8 min crosslinked G-P NF in different pH (1.2, 6, 7.4 and 8).

For crosslinking time of 4 min (G-PNF 4), piperine release percentage was 95.7%, 90.52%, 82.76%, 77.76% (figure 3.5.a) while for crosslinking time of 6 min (G-PNF 6), drug release percentage was 87.70%, 85.57%, 77.56% and 72.56% for pH 8, pH 7.4, pH 6 and pH 1.2 respectively (figure 3.5.b). We observe that the total amount of drug release is less in the solution with pH 1.2 compared to higher pH, irrespective of crosslinking

time. This may be due to protonation of hydrophilic groups of the polymer matrix in acidic pH, leading to collapse state of the membrane. It discourages formation of H-bonds with water molecules and results in less swelling of the membrane<sup>28</sup>. If the matrix is not swelling much, drug molecules will not get enough osmotic pressure to be released in medium, helping in reducing drug release amount. However in alkaline pH, hydrophilic groups form more H-bonds with release medium which invites more water molecules inside the carrier leading to better swelling and more drug release in the dissolution medium. Similarly, for 8 min crosslinking, after 24 h, piperine release was 72.70%, 65.51%, 62.56% and 58.56%, for pH 8, pH 7.4, pH 6 and pH 1.2 respectively, demonstrating the above explanation.

### ***3.3.6.2 Effect of crosslinking time***

With increasing the crosslinking time from 6 to 8 min, the large amount of drug release in pH 1.2 can be controlled. Our main objective is to release maximum drug in higher pH (7.4, 8) i.e. pH of small intestine, where drug will be absorbed. In release medium of pH 1.2, the amount of drug release, within 2 h, for G-PNF 4, G-PNF 6 and G-PNF 8 are approximately 48.5%, 45.5% and 30.5% of total drug respectively (figure 3.6.a). Further, the drug release amount decreases from 72.6% in G-PNF 6 to 58.5% in G-PNF 8, after 24h release. Therefore, increasing crosslinking time, decreases the release percentage.

Similar control over the release percentage was obtained for pH 6, pH 7.4 and pH 8 for both initial fast release and prolonged sustained release as shown in figure 3.6.b-d. Therefore, manipulating the crosslinking exposure time from 4 to 8 min, we can engineer the inter-fibrous porosity, which may result in sustained release of drug molecules. Also, from release study we can conclude that, the vehicle is capable of protecting the drug from the harsh condition (pH 1.2) of GI tract and is able to release in the absorption site, i.e., small intestine, in a sustained manner.

Therefore, in-vitro drug release study suggests that crosslinking plays very important role in porosity of the matrix, which actually helps to get stable, sustained and control release of drug with highly porous nanofiber matrix as a delivery vehicle.

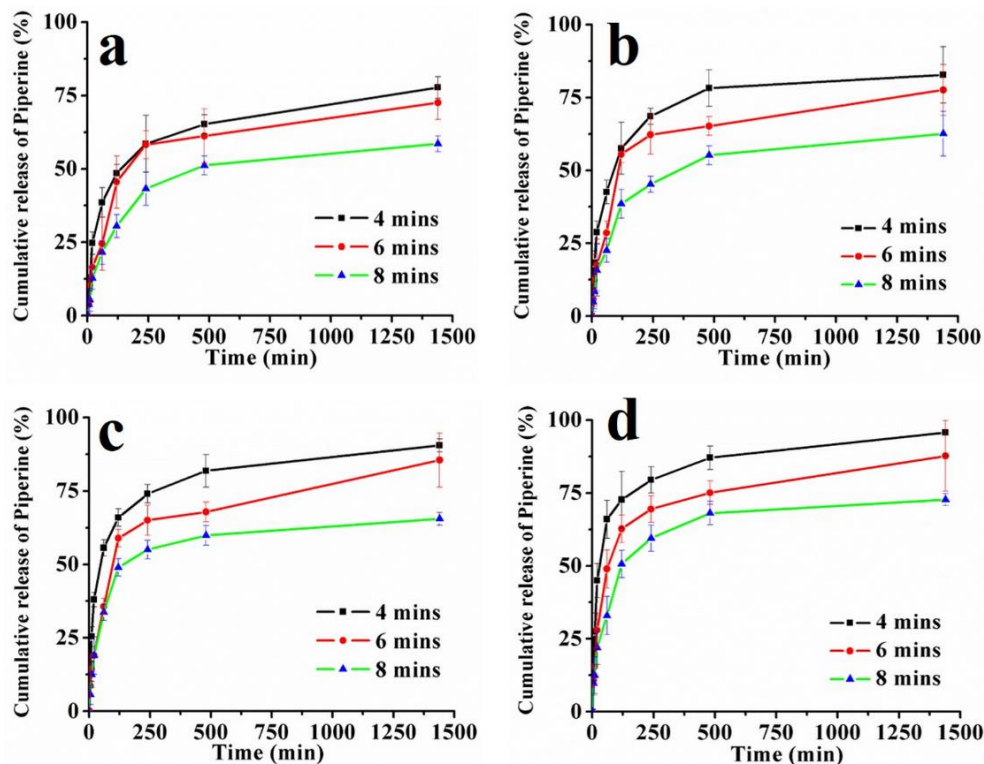


**Figure 3.6** Cumulative release of piperine for different crosslinking time in (a) pH 1.2. (b) pH 6 (c) pH 7.4, and (d) pH 8.

### 3.4 Conclusions

Electrospun gelatin nanofibers were fabricated and exposed to saturated GTA (25% v/v) vapour for crosslinking. Interestingly, only 6 min exposure was sufficient to maintain the morphology of nanofibers when tested by soaking in different pH for 24 h. Besides increasing water resistivity, crosslinking also improved the thermal stability of membrane. These electrospun gelatin fibers were then successfully demonstrated as a carrier for hydrophobic drug i.e, piperine. This system have the potential in drug delivery system due to following observations: (i) piperine was found to be stable in hydrophilic electrospun gelatin nanofiber carrier, with and without crosslinking with GTA vapour; (ii) From in vitro release study, piperine was effectively delivered over prolonged duration of release; (iii) piperine release rate can be modulated by pH of the release medium at the site of release and the degree of cross-linking of the carrier.

### 3.5 Acknowledgements

We acknowledge Dr(s). Prabu Sankar and Pinaki Prasad Bhattacharjee for their help in FTIR/ATR and FESEM analysis.

## References

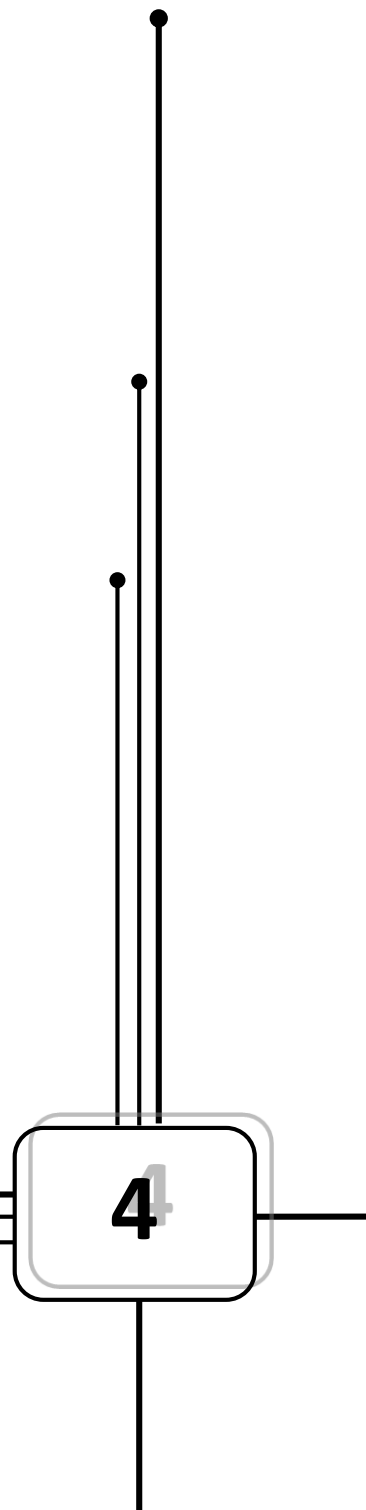
1. D. Pailino, M. Fresta, P. Sinha, M. Ferrari, Encyclopedia of medical devices and instrumentation, Second Edition, John G. Webster (Ed.), John Wiley & Sons, Inc. 2006.
2. R.P Dixit, S.P Puthli, Oral strip technology: Overview and future potential, *J. Controlled Release* 139 (2009) 94–107.
3. A. Kumari, S.K Yadav, S.C Yadav, Biodegradable polymeric nanoparticles based drug delivery systems, *Colloids Surf., B* 75 (2010) 1–18.
4. L. Zhou, F. Zhang, Thermo-sensitive and photoluminescent hydrogels: Synthesis, characterization, and their drug-release property, *Mater. Sci. Eng. C* 31 (2011)1429–1435.
5. T.R Hoare, D.S Kohane, Hydrogels in drug delivery: Progress and challenges, *Polymer* 49 (2008) 1993-2007.
6. W. Yan, V.K.S. Hsiao, Y.B. Zheng, Y.M. Shariff, T. Gao, T.J. Huang, Towards nanoporous polymer thin film-based drug delivery systems, *Thin Solid Films* 517 (2009) 1794–1798.
7. F. Siepmann, C. Wahle, B. Leclercq, B. Carlin, J. Siepmann, pH-sensitive film coatings: Towards a better understanding and facilitated optimization. *Eur. J. Pharm. Biopharm.* 68 (2008) 2–10.
8. A.S. Narang, D. Delmarre, D. Gao, Stable drug encapsulation in micelles and microemulsions. *Int. J. Pharm.* 345 (2007) 9–25.
9. L. Wei, C. Cai, J. Lin, T. Chen, Dual-drug delivery system based on hydrogel/micelle composites, *Biomaterials* 30 (2009) 2606–2613.
10. J.K. Oh, D.I. Leea, J.M. Park, Biopolymer-based microgels/nanogels for drug delivery applications, *Prog. Polym. Sci* 34 (2009) 1261–1282.
11. M. Malmsten, H. Bysell, P. Hansson, Biomacromolecules in microgels-Opportunities and challenges for drug delivery. *Curr. Opin. Colloid Interface Sci.* 15 (2010) 435–444.
12. Z.M. Huang, Y.Z. Zhang, M. Kotaki, S. Ramakrishna, A review on polymer nano-fibers by electrospinning and their applications in nanocomposites, *Compos. Sci. Technol.* 63 (2003) 2223–2253.
13. S. Ramakrishna, K. Fujihara, W.E. Teo, T.C. Lim, Z. Ma, An Introduction to Electrospinning and Nano-fibers, World Scientific Publishing Co. Pte. Ltd.2005.
14. D.B. Khadka, D.T. Haynie, Protein- and peptide-based electrospun nano-fibers in medical biomaterials, *Nanomed. Nanotech. Biol. Med.* 8 (2012)1242–1262.

15. S.Young, M. Wong, Y. Tabata , A.G. Mikos, Gelatin as a delivery vehicle for the controlled release of bioactive molecules, *J. Controlled Release* 109 (2005) 256– 274.
16. E.J. Chong , T.T. Phan, I.J. Lim , Y.Z. Zhang , B.H. Bay , S. Ramakrishna , C.T. Lim, Evaluation of electrospun PCL/gelatin nanofibrous scaffold for wound healing and layered dermal reconstitution, *Acta Biomater.* 3 (2007) 321–330.
17. R.S. Tigli, N.M. Kazaroglu, B.Mavis, M. Gumusderelioglu, Cellular Behavior on Epidermal Growth Factor (EGF)-Immobilized PCL/Gelatin Nanofibrous Scaffolds, *J. Biomater. Sci.* 22 (2011) 207–223.
18. S. Gautam, A.K. Dinda, N.C. Mishra, Fabrication and characterization of PCL/gelatin composite nanofibrous scaffold for tissue engineering applications by electrospinning method, *Mater. Sci. Eng. C* 33 (2013) 1228–1235.
19. S. Gautam, C.F. Chou, A.K. Dinda, P.D.Potdar, N.C. Mishra, Surface modification of nanofibrous polycaprolactone/gelatin composite scaffold by collagen type I grafting for skin tissue engineering, *Mater. Sci. Eng. C* 34 (2014) 402–409.
20. D. Yang, Y. Li, J. Nie, Preparation of gelatin/PVA nanofibers and their potential application in controlled release of drugs, *Carbohydr. Polym.* 69 (2007) 538–543.
21. Y.Z. Zhang, J. Venugopal, Z.M. Huang, C.T. Lim, S. Ramakrishna, Crosslinking of the electrospun gelatin nanofibers. *Polymer* 47 (2006) 2911–2917.
22. R.A. Carvalho, C.R.F. Grosso, Characterization of gelatin based films modified with transglutaminase, glyoxal and formaldehyde, *Food Hydrocolloid* 18 (2004) 717–726.
23. A. Bigi, G. Cojazzi, S. Panzavolta, N. Roveri, K. Rubini, Stabilization of gelatin films by crosslinking with genipin, *Biomaterials* 23 (2002) 4827–4832.
24. S. Farris, J. Song, Q. Huang, Alternative Reaction Mechanism for the Cross-Linking of Gelatin with Glutaraldehyde, *J. Agric. Food Chem.* 58 (2010) No. 2.
25. N. Ahmad, H. Fazal, B.H. Abbasi, S. Farooq, M. Ali, M.A Mubarak Ali Khan, Biological role of Piper nigrum L. (Black pepper): A review, *Asian Pac. J. Trop. Biomed.* (2012) 1945-1953.
26. G. Shoba, D. Joy, T. Joseph, M. Majeed, R. Rajendran, P.S.S.R. Srinivas, Influence of Piperine on the Pharmacokinetics of Curcumin in Animals and Human Volunteers, *Planta Med.* 64(4) (1998) 353-356.
27. M.A. Oraby, A.I. Waley, A.I.E. Dewany, E.A. Saad, Abd El-Hady Bothaina, Electrospun Gelatin Nanofibers: Effect of Gelatin Concentration on Morphology and Fiber Diameters, *J Appl. Sci. Res.* 9(1) (2013) 534-540.

28. K. Jalaja, P.R.A. Kumar, T. Dey, S.C. Kundu, N.R. James, Modified dextran cross-linked electrospun gelatin nanofibres for biomedical applications, *Carbohydr. Polym.* 114 (2014) 467-475.



**Orange Peel Extract  
as Natural Transfer Solution  
for Print Transfer Technique**



## **Abstract**

Orange peels are the waste products in most of the juice industries and are categorized as solid waste. However, these orange peels are rich in component, which are extracted using distillation or solvent extraction. These components are widely used in many applications such as in pharmaceuticals, perfume industry etc. In this work, we are preparing extract from orange peel by very easy and inexpensive method. The extract will be used directly, without further separation of components. The components present were then identified using GC-MS analysis. Further, the orange peel extract was used as a natural transfer solution for print transfer method, which is advantageous in terms of cost, availability and non-toxicity of the transfer solution.

## 4.1 Introduction

Oranges find its main application in juice industries. The thick bitter peels are removed in the process of making juice. These discarded peels are difficult to dispose and are categorized as solid agricultural waste<sup>1</sup>.

Orange peels can be processed into animal feed by desiccation, using pressure and heat<sup>2</sup>. Orange oil can be obtained by pressing the peel and is the by-product of juice industry which is used for flavouring food and for imparting fragrance in perfume industry. These peels are used as adsorbents in industries for removal of dyes, water contaminants and pollutants etc.<sup>3-5</sup> Moreover, orange peel is edible and has higher Vitamin- C content<sup>2</sup>. The peel of orange is rich in many components such as

1. limonene that is used in cosmetics, perfume industry, flavouring of food, insecticides, as a solvent and as a household cleaner;
2. pectin that is used in cosmetics, pharmaceuticals and in food like jellies;
3.  $\alpha$ -Pinene which is anti-inflammatory in nature; and
4. other components such as myrcene, linalool etc.<sup>6</sup>

The extraction of these components is either done by distillation, cold pressing or solvent extraction<sup>7</sup>.

In this work, we present a very simple process of preparing extract from orange peel and using it without further separation of components. The components present were then identified using GC-MS analysis and solution properties such as surface tension, viscosity and conductivity were measured. This extract prepared will be then further used as a transfer solution for print transfer technique, on different substrates such as paper, cloth, nail and skin.

Print transfer method is used for making beautiful patterns or artistic designs on cloth, fabric, paper, walls etc. in order to enhance the appearance of respective objects creatively. Accordingly, different arts such as nail art, tattoos, cloth printing, paper printing etc.<sup>8-9</sup> are well established. Many solutions, such as isopropyl alcohol, acetone, etc.<sup>10</sup> are used as the transfer solution for transferring print on the substrate from the template/pattern in the print transfer technique. Citra-solv is well known commercial product, with limonene as its main component, used as natural transfer solution<sup>9</sup>. However, all these transfer solution are known to be toxic and harmful if concentrated or overused. Therefore, the use of orange peel extract as the transfer solution is advantageous because it is non-toxic, can be easily prepared and inexpensive as it is from waste orange peel.

## 4.2 Experimental methods

### 4.2.1 Materials

Oranges were purchased from local market of Hyderabad.

### 4.2.2 Preparation of extract

Oranges were washed with water, in order to remove any dirt particles on the peel. Peel was then removed using knife (figure 4.1.a) or simply by hand. It should have the white layer present beneath the outer rind of peel (figure 4.1.b). When the peel was folded and pressed, then a liquid spray comes out of the outer rind of peel (figure 4.1.c). This spray was collected (figure 4.1.d) and named as the primary extract (PE).

When the primary extract was allowed to settle, or centrifuged, then it separates into three layers, as shown in figure 4.1.e. According to the order from top to bottom, these layers are named as top layer (TL), middle layer (ML) and bottom layer (BL) respectively.

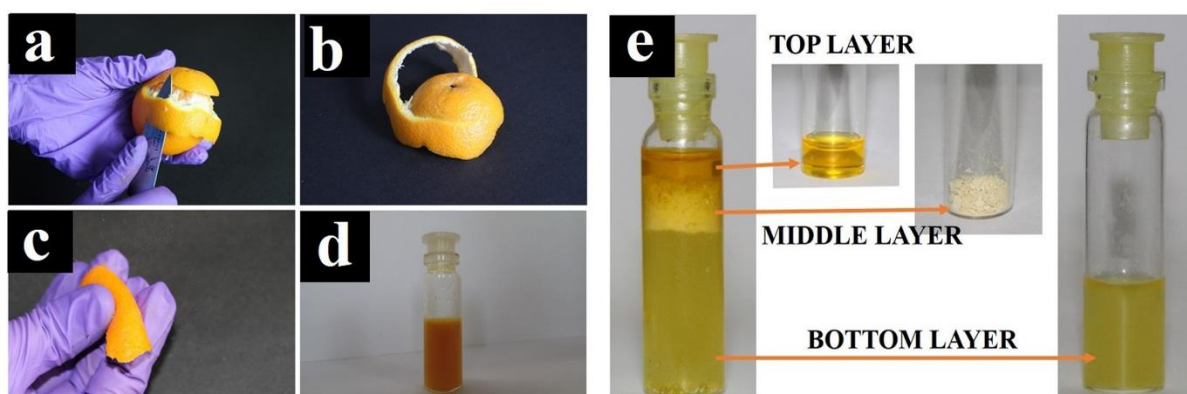


**Figure 4.1** Different steps for preparing primary extract from the orange peel (a-d); layers in primary extract (e)

### 4.2.3 Gas chromatography-mass spectroscopy (GCMS) analysis

The components of top layer were identified using GC attached with mass spectroscopy (Shimadzu, GCMS-QP2010 Ultra). The products were quantified by GC (Shimadzu, GC-2014) using capillary column (ZB-5HT Inferno, Phenomenex, 30 m 0.32 mm 0.10 mm) connected with flame ionization detector (FID). The following GC oven temperature programming was used to obtain well resolved chromatogram: Initially oven was kept at 50<sup>0</sup> C for 5 minutes and then temperature was increased to 250<sup>0</sup> C with a ramping rate of 20<sup>0</sup> C / min. Injector and

detector were maintained at 260<sup>0</sup> C and 280<sup>0</sup> C respectively. It was held at this temperature for 5 min.

#### 4.2.4 Conductivity

The electrical conductivity of all layers were measured using a conductometer (HI 2300 EC/TDS/NaCl Meter , HANNA INSTRUMENT ) at room temperature in triplicates.

#### 4.2.5 Surface tension

The surface tensions of the solutions were measured by goniometer (Ramé-hart instrument co., Model 290 F4 series)

#### 4.2.6 Viscosity

The viscosity of layers were measured by using (Brookfield Viscometer DV-11+ Pro) viscometer and confirmed by rheometer ( Haakemars III)

#### 4.2.7 Print transfer method

The print out of the desired pattern or designs in form of characters, figures etc. was taken and referred as template. This template is then used to the transfer or stick characters, figures etc. on different substrates. Substrates selected are paper, cotton cloth, nail and human skin (tattoo).

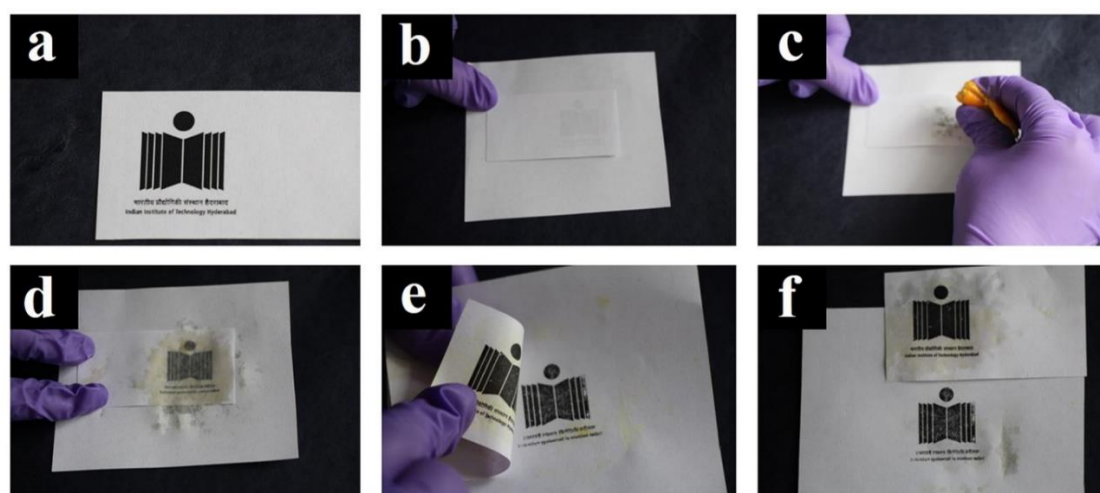


**Figure 4.2** (a) Template and print transfer using orange peel extract (b-f) on paper.

Take the template (figure 4.2.a) and place it on the substrate upside down (figure 4.2.b). Squeeze the orange peel directly on the template (figure 4.2.c) or spread the primary extract on

the template using brush. Then allow it to dry (figure 4.2.d) and remove it carefully as shown in figure 4.2.e. The same results of print transfer were obtained when only TL was used as the transfer solution.

## 4.3 Results and Discussion

### 4.3.1 GC-MS analysis

Figure 4.3 represents the gas chromatograph of top layer and components identified for the respective peaks. As can be seen d-limonene is the major component in the TL while,  $\beta$ -myrcene and  $\gamma$ -terpinene are present in comparable amount (fig 3.a). The fractions of 2- $\beta$ -pinene, 2-carene, linalool, decanal,  $\delta$ -elemene, germacrene and  $\gamma$ -elemene were also found to be present in TL.

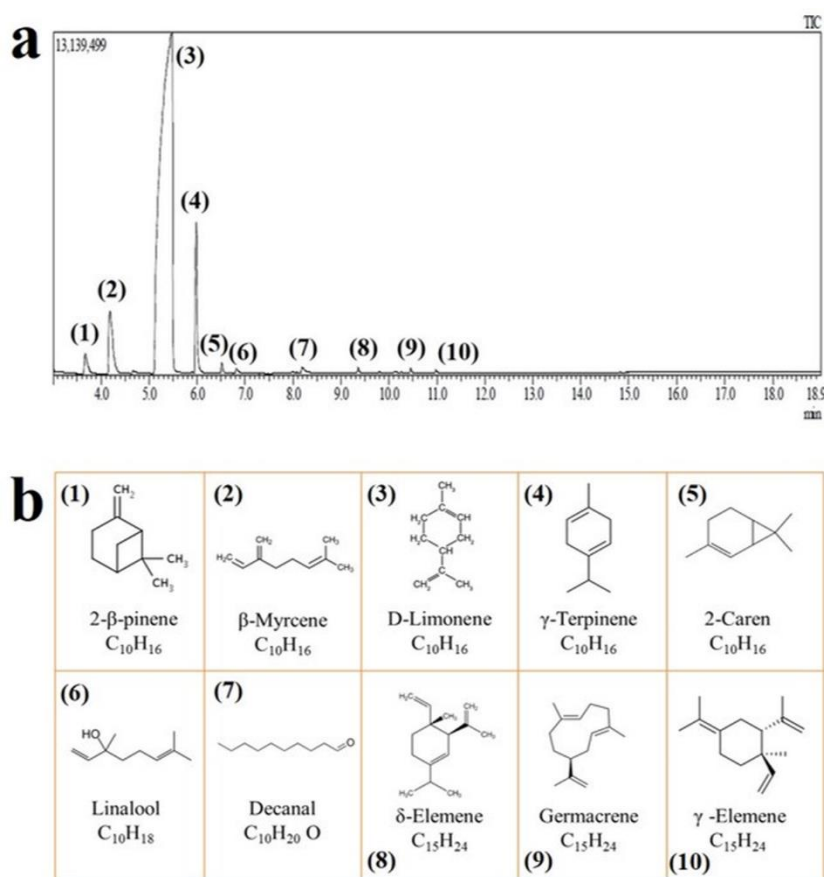


**Figure 4.3.** (a) Gas chromatograph of TL, (b) Identified components corresponding to each peak in gas chromatograph

### 4.3.2 Solution properties

Primary extract (PE) was separated into three layers by gravity settling or centrifuging. Middle layer (ML) constitutes mainly solid particles and therefore separated. Measured properties of top layer and bottom layer are tabulated in table 4.1.

**Table 4.1** Properties of top and bottom layer of PE

Property	Top layer	Bottom layer
Conductivity	0.00 $\mu$ S	3.44 mS
Surface tension	27.81 mN/m	41.72 mN/m
Viscosity	0.79 cP	0.43 cP

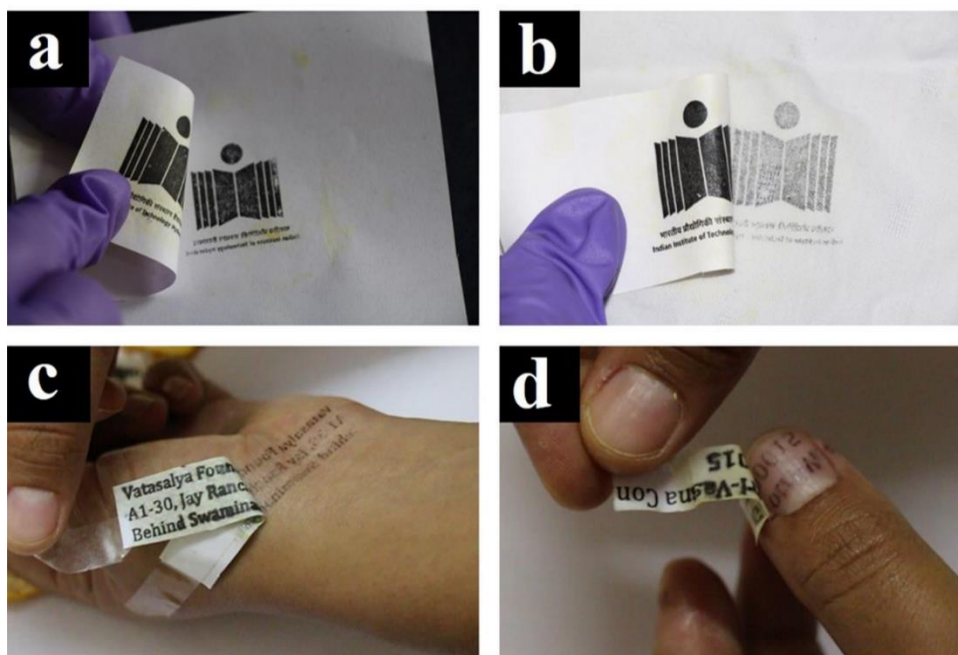
### 4.3.3 Print transfer method

Figure 4.2 illustrates the method of print transferring using primary extract from orange peel on paper. Limonene is the major component of the extract and is known to be responsible for the transfer of print. The extract separates the ink from the template by deteriorating an adhesive force between ink and paper of template and sticking the ink on the substrate used. It can be seen that squeezing orange peel directly or using the primary extract, not only simplifies the process but also makes it user friendly. It also adds the advantage of being natural transfer solution along with using waste orange peel skillfully.

Figure 4.4 shows the various substrates, on which print can be transferred. Paper (figure 4.4.a) and cloth (figure 4.4.b) are most commonly used materials in our day-to-day life. This method is very handy and therefore, can be used for transferring different patterns on these substrates easily.

There are lot of people who like getting their body inked with different designs as per the latest trend. However permanent tattoos have the disadvantages like allergies, infection on sensitive skin, lot of after care and more importantly designs cannot be changed. Therefore many people make temporary design on skin using markers, liners etc. For the design to look good, consumer has to practice it and this limits the use of these tattoo. With the print transfer method, consumer can take the print out of the required design and use it as a template. Figure 4.4.c shows the transfer of characters on hand by following steps as shown in figure 4.2. Therefore, primary extract can be used for transferring print on skin, i.e, making temporary tattoo.

Nail art is also a way of exhibiting different colors and patterns on nails depending on the lifestyle. Nowadays, use of different patterns on nails are gaining popularity over solid colors. The patterns can be printed materials, figures, characters, newspaper arts etc. By following the steps as shown in figure 4.2, we can transfer print on nail easily, just by squeezing orange peel on the template. Figure 4.4.d represents an example of transferring characters on nail, without applying any base coat. Specifically, base coat is not required but, can be kept to make the art more attractive.



**Figure 4.4** Print transfer on substrates (a) paper (b) cotton cloth (c) skin and (d) nail

Further, these patterns obtained are stable against water and rubbing. Therefore, extract from orange peel is user friendly, natural, inexpensive transfer solution, produced from waste orange peels.

#### 4.4 Conclusion

The method used for the preparation of orange peel extract is very simple and cost effective. The orange peel constitutes numerous valuable compounds which are found to be present in the extract prepared in this work. This extract was then successfully used as a transfer solution in print transfer on paper, cloth, nail and skin, without further processing of the solution. Further, only TL can also be used as transfer solution. Therefore, this method is advantageous in terms of extraction of solution from orange peel and handy print-transfer method. Also, the transfer solution is completely natural and inexpensive. Therefore, extract can be prepared and used at home and can be scaled to industrial level, using waste orange peel creatively.



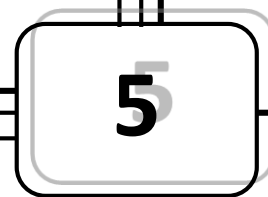
#### **4.5 Acknowledgements**

We would like to thank Mrunalini Gaydhane and Srinadh Mattaparthi for their help and suggestions for this work.

## References

1. Jarrell, A. Squeezing oranges to reduce waste, Inside Science News Service, June 13, 2015, Website. <http://www.insidescience.org/content/squeezing-oranges-reduce-waste/732>
2. Website. [https://en.wikipedia.org/wiki/Orange\\_\(fruit\)](https://en.wikipedia.org/wiki/Orange_(fruit))
3. C. Namasivayam, N. Muniasamy, K. Gayatri, M. Rani, K. Ranganathan. Removal of dyes from aqueous solutions by cellulosic waste orange peel. *Bioresource Technology* 57 (1996) 37-43
4. M. R. Fat'hi, A. Zolfi. Removal of Blue 56 by Orange Peel from the Waste Water. *Journal of Chemical Health Risks* 2(1) (2012), 7-14
5. F. B. AbdurRahman, M. Akter, M. Zainal Abedin. Dyes Removal From Textile Wastewater Using Orange Peels. *International journal of scientific & technology*, 47 (2013), 2277-8616
6. Website [https://en.wikipedia.org/wiki/Orange\\_oil](https://en.wikipedia.org/wiki/Orange_oil)
7. Sawamura, M. Citrus essential oil. A John Wiley and Sons, Inc. Publications.: Singapore, 2010
8. Hye Sun IM, Transfer Solution for Nail Printing and nail printing method using the same. US 2014/0060349, March 6, 2014.
9. Website. <http://www.instructables.com/id/Fabric-Printing-with-Citra-Solv>
10. Website <http://www.instructables.com/id/Solvent-Transfers/>

**Recycled Polystyrene based  
Sub-micron Aligned Fibers using  
Orange Peel Extract for Oil  
Spill Remediation**



## **Abstract**

We report here novel and innovative way of producing sub-micron, aligned fibers from objects made up of polystyrene, with controllable geometry, from extract obtained from peel of orange fruit. The process depicted here for the fabrication is not only facile, flexible but at the same time versatile with minimum requirements for making aligned fibers. The fibers produced were then characterised in terms of surface morphology, crystal size, surface area, thermal stability and wettability behavior. The fibers were found to be hydrophobic and oleophilic in nature. Based on this property, these fibers were then tested as a sorbent material for oil. The absorption capacity of fibers prepared using primary extract was about  $23.8 \pm 2$  g/g and  $12.9 \pm 1.8$  g/g with coconut and mustard oil respectively, which got increased to  $30.7 \pm 0.4$  g/g to  $40.5 \pm 3.6$  g/g respectively when fibers were prepared using only top layer of primary extract. Further tests were done to quantify the retention capacity and reusability of fibers and it was found that these fibers have great potential to be used as sorbent material for oil.

## **5.1 Introduction**

Polystyrene (PS) is one of the most widely used thermoplastic polymer<sup>1</sup>. It is used as solid PS in applications such as electronics, construction, house and medical ware, disposal food services etc. Whereas, for protective packaging, in electrical, pharmaceutical and retail industries etc., it is used in form of foam, because of its light weight, shock resistance, cushioning properties, and flexibility in design possibilities<sup>2-3</sup>. But PS comes with the disadvantage of being non-biodegradable<sup>3</sup> and therefore, raises concern over its impact on health and environment. PS is major component of plastic debris in ocean, where it becomes hazardous to marine life. Also, Styrofoam blows in wind and floats on water, making it difficult to collect and control the waste<sup>2</sup>. PS packaging products are usually discarded in dumps, landfills or simple litter after their useful application<sup>2</sup>. As the waste plastic material has become a serious problem, recycling is getting attention to save environment and resource recovery.

The three main alternatives for PS recycling are, mechanical, chemical and thermal recycling<sup>3</sup>. Mechanical recycling involves relatively simple technologies for converting scrap PS into new product, by compressing and melting. But it can be quite labour- or energy-intensive, depending on whether the process is manual or automated. Chemical recycling can have high capital cost such as in catalytic degradation of PS. whereas, toxic emission in thermal recycling refrains its use<sup>1</sup>. All recycling methods involves energy input as the preliminary step either to crush PS objects into granules or thermally degrade them.

In this work we present a novel and innovative way to recycle objects made up of PS directly into sub-micron, aligned PS fibers using citrus fruit's peel extract. The fibers produced were then characterised in terms of surface morphology, crystal size, surface area, thermal stability and wettability behaviour. The fibers were found to be hydrophobic and oleophilic. Based on this property, these fibers were then tested as a sorbent material for oil. Further tests were done to quantify the retention capacity and reusability of fibers. Buoyancy test was also done to check if fibers floats on water after absorption of oil and and it was found that these fibers have great potential to be used as sorbent material for oil.

## **5.2 Experimental methods**

### **5.2.1 Materials**

Geometric scale, oranges, mustard oil and coconut oil (Parachute, Marico Ltd.) were bought from local market of Hyderabad. PS with molecular weight (Mw) 3, 50,000

g/mol was purchased from Sigma Aldrich. DMF (99% purity) and THF (99% purity) were purchased from Merck India. Deionized water (DI) (Milli Q, resistivity 18.1 M $\Omega$ .cm) were used throughout the experiments. All the chemicals were used without further purification.

### 5.2.2 Orange peel extract

The orange peel extract was prepared as mentioned in chapter 4. The primary extract (PE) or top layer (TL) are used for making fibers.

### 5.2.3 Preparation of fibers

Figure 1 illustrates the step wise procedure of fabrication of sub-micron fibers from geometric scale which is made up of PS. Figure 5.1.a shows the requirements for the process, which includes orange peel, hand, scale and substrate to deposit fibers. Following are the steps:

1. Squeeze the orange peel or take few drops of PE on palm (figure 5.1.b)
2. Then take scale and press it on the palm where sample was sprayed as shown in figure 5.1.c
3. Pull the scale horizontally away from hand or palm (figure 5.1.d).
4. Figure 5.1.e shows the drawn fibers obtained from the method.
5. Take fibers towards / on the substrate or object where it is to be deposited, here it is cylindrical beaker as shown in figure 5.1.f.
6. The fibers are placed carefully on the beaker as in figure 5.1.g to obtain horizontal alignment of the fibers (figure 5.1.h).
7. The steps from 2-6 are repeated till extract dries and then put then extract again on hand (step 1) This will be referred as cycle 1.
8. Repeat cycles the desired thickness or geometry of the fiber is obtained.
9. Similarly different geometries of the fibers can be obtained as shown in figure 5.1.i – j. This method is similar to drawing method and therefore, geometry of the fibers prepared can be easily controlled by changing the direction or angle while depositing the drawn fibers.

Therefore, fibers prepared using primary extract and top layer are referred as PEF and TLF respectively. Further, citrus fruit's peel such as, lemon peel, kinnow peel and mosambi peel etc. can also be used to recycle PS into fibers.

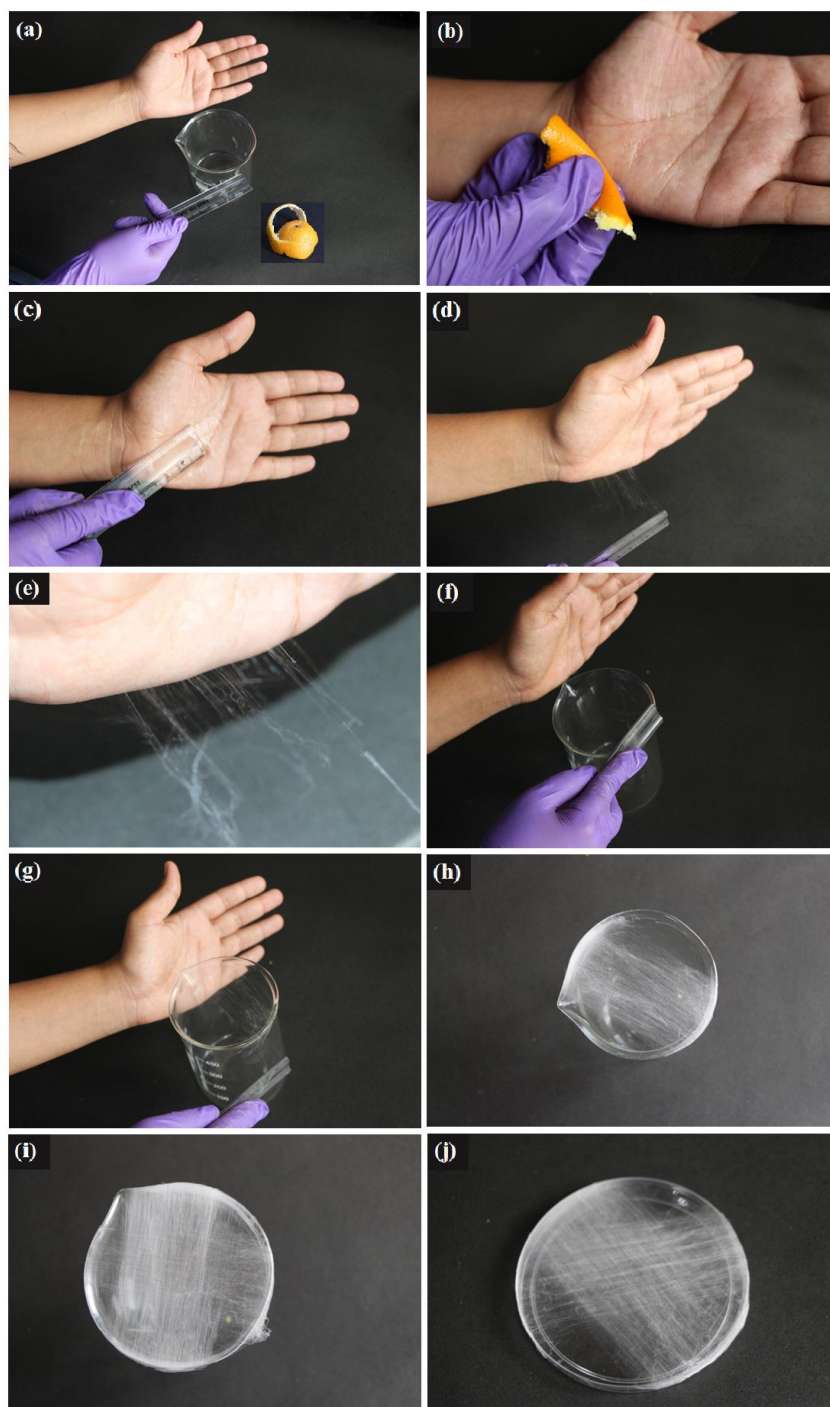


**Figure 5.1** Materials required (a) and steps of drawing fibers from geometric scale (b-h); fibers aligned at  $90^{\circ}$  (i) and  $45^{\circ}$  (j).

## 5.2.4 Electrospun PS fibers

### 5.2.4.1 Preparation of solution

A 14 wt. % PS solution was prepared by dissolving PS in DMF-THF solvent mixture of 70:30 at  $50^{\circ}\text{C}$  using a magnetic stirrer.

#### **5.2.4.2 Electrospinning**

PS solution in DMF:THF of 70:30 was electrospun in electrospinning set up (E-spin Nanotech Pvt. Ltd. (India)). Size of the needle, applied voltage and the distance between the needle and the collector (Al foil) were some of the process parameters that were optimized in this study to obtain long, continuous and uniform fibers. These parameters were as follows: 23 gauge syringe needle, 12kV applied voltage and 8cm. All the experiments were conducted at a temperature of 35 °C.

#### **5.2.5 Morphological characterization**

The surface morphologies of the recycled PS fibers and electrospun PS fibers were observed by using scanning electron microscopy (SEM) (Phenom world). All samples were sputtered with thin layer of gold before image analysis in SEM.

#### **5.2.6 Specific surface area (SSA) measurement**

The Brunauer–Emmett–Teller (BET) surface area of PEF, TLF and espun PSF was determined by N<sub>2</sub> physisorption using Quantachrome instruments v3.01. The weight of the sample was fixed to be 100 mg. All samples were degassed at 80<sup>0</sup> C for 60 min in nitrogen. The SSAs were determined by a multi-point BET measurement with nitrogen as the adsorbate.

#### **5.2.7 FTIR/ATR Spectroscopy**

PEF, TLF and espun PSF were characterized by using Fourier transform infrared (FTIR) spectrometer (Bruker Alpha-P) in 500-4000 cm<sup>-1</sup> range

#### **5.2.8 X-ray diffraction analysis**

Powder X-ray measurements were recorded in scattering angle range of 10° to 60° on PANalytical X-ray diffractometer with CuK $\alpha$  radiation to study the crystallinity of the sample

#### **5.2.9 Contact angle measurement**

Contact angles were measured by goniometer (Ramé-hart instrument co., Model 290 F4 series) by image processing of sessile drop with a DROImage Advanced software. Drops of purified water, 3  $\mu$ l, were deposited on the surface to form sessile drop using a micro-syringe attached to the goniometer. Contact angles on different parts of films were measured and averaged.



### 5.2.9 Thermogravimetric analysis

Thermogravimetric analysis (TGA) of PEF, TLF and espun PSF samples was carried out using platinum pan in argon atmosphere (pyris 1, Thermogravimetric analyser, Perkin Elmer). Sample weight varies from 5 to 10 mg and samples were heated from room temperature to 900 °C at a heating rate of 5 °C/min.

### 5.2.10 Oils used

Mustard oil and coconut oil are selected to tests the prepared PEF and TLF and as-spun PSF for sorbent for oil. Table 5.1 illustrates the properties of these oils.

**Table 5.1** Properties of mustard oil and coconut oil

Properties	Mustard oil	Coconut oil
Viscosity	56.5 cP	17.24 cP
Density	0.9180 g/cm <sup>3</sup>	0.9260 g/cm <sup>3</sup>

### 5.2.11 Absorption method<sup>4</sup>

Approximately 0.2g of sample was weighed and kept in glass beaker containing 100mL of oil. The sample were taken out after 60 min and excess oil was drained for 2 min. If initial weight of the sample is  $W_i$  and weight after draining excess oil is  $W_0$ , then the percent oil absorption capacity (Q) of sample is given by:

$$Q = [(W_0 - W_i) / W_i] * 100$$

For all samples, tests were repeated three times independently and average values with standard deviation were calculated.

### 5.2.12 Retention test<sup>5</sup>

The desorption rate of oil from sorbed fibers due to gravity, was examined with respect to time, i.e., weight loss from the sample was measured after 10, 20,30,40,50 and 60 min respectively.

### **5.2.13 Reusability test<sup>5</sup>**

The sorbed fibers were squeezed by applying pressure and all the oil was removed. Then sample was allowed to absorb oil again for 60 min, and absorption capacity was measured for this second cycle. Repeat the cycle 5 times and measure the difference in absorption capacity after 5 cycles. For all samples, tests were repeated three times independently and average values with standard deviation were calculated.

### **5.2.14 Buoyancy test<sup>4</sup>**

Buoyancy test was carried out in two systems. In static system, 10 ml of oil was poured into glass beaker containing 200 mL of water. About 0.3 g of fibers was carefully kept on the surface. In dynamic system, is similar to static system, but there is continuous stirring (300 rpm) by magnetic stirrer.

## **5.3 Results and discussion**

### **5.3.1 Drawing of fibers from PS objects**

Procedure of recycling geometric scale into sub-micron fibers, is mentioned above and illustrated in figure 5.1. The major component of primary extract or TL is limonene as identified in GC-MS analysis (chapter 4). D-Limonene is well known solvent for dissolving expanded PS or Styrofoam<sup>6-7</sup>. Therefore, when scale comes in contact with PE or TL, it starts getting dissolved in the solution. It forms a thick solution at the surface of scale. Solution is part of surface of scale and it adhere to hand when scale is pressed against hand. When scale is pulled outward, the solution stretches into fibers. Figure 5.2.a shows that fibers are attached to both scale and hand surface. Figure 5.2.b shows the degradation of scale used for making fibers. In figure 5.2.b (i) is the original scale which degrades using PEF and TLF as shown in figure 5.2.b (ii) and 5.2.b (iii) respectively. In case of using PE for making fibers, the particles of ML starts depositing on scale (figure 5.2.b (ii)) making it sticky in nature, which can be avoided if only TL is used.

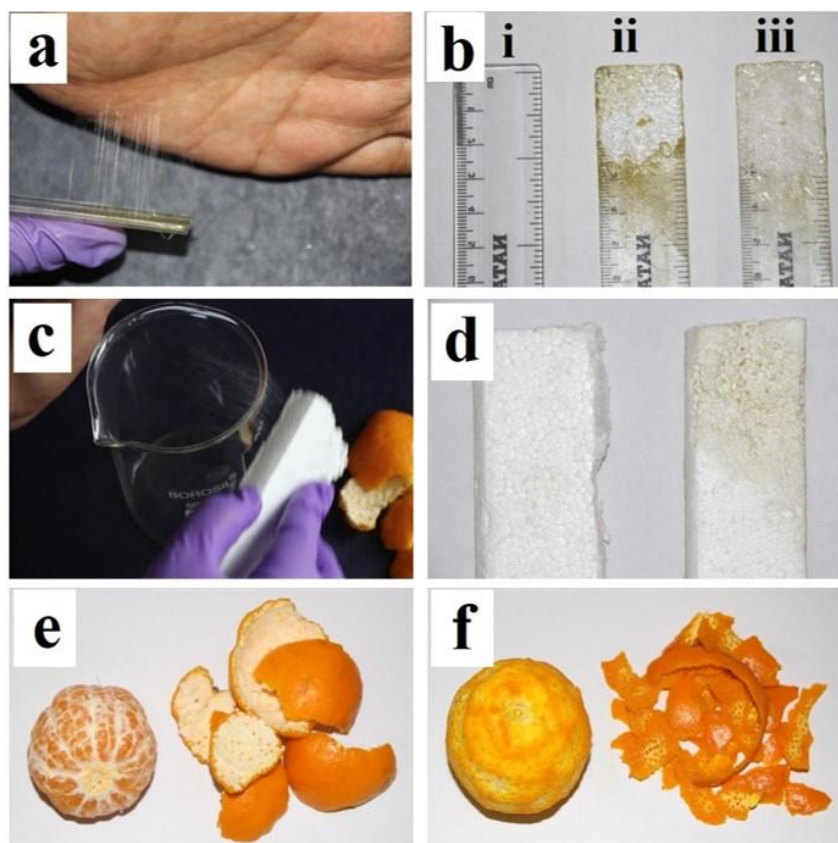


**Figure 5.2** (a) Fibers between hand and scale, (b) degradation of scale after deposition, (c) fibers from thermocol, (d) degradation of thermocol; ways of peel orange (e-f)

Similarly, fibers can be prepared from thermocol, one of the form of polystyrene, which light weight and mainly used for packaging. Figure 5.2.c and 5.2.d represents fibers from thermocol deposited on beaker and degradation of thermocol surface as it dissolves in orange peel extract.

In general, for extracting components from orange peel, the peels are taken out as shown in figure 5.2.f. It is then either processed by distillation or solvent extraction and in both the cases the white material beneath the outer layer of peel is not required. In our method, this white layer prevents the breakage of peel on folding and squeezing. Therefore, we use peels as shown in figure 5.2.e.

Approximate weight of peel of one medium sized (5-6 cm diameter) orange as in figure 5.2.e is 20-25 g. From such oranges, about 5 mL of PE gets collected. When this 5 mL PE was centrifuged, approximately 1mL of TL gets collected. In case of drawing fibers from scale, 1 mL of TL gives about 200 -25 mg of TLF.

### 5.3.1 Surface Morphology

Surface morphology of the fibers prepared is shown in figure 5.3. The fibers made using primary extract i.e, PEF are aligned and yellowish in color (figure 5.3.a) as the ML particles are also present in mat; whereas TLF are white in color (figure 5.3.b). Scanning Electron Microscope (SEM) analysis was done to study the morphology of recycled PS fibers prepared using orange peel extract and electrospun PS fibers. Recycled PS fibers were aligned as shown in figure 5.3.c and 5.3.d, i.e., prepared using primary extract and top layer respectively. The diameter of fibers i.e., PEF and TLF varies from 1-10  $\mu\text{m}$ .

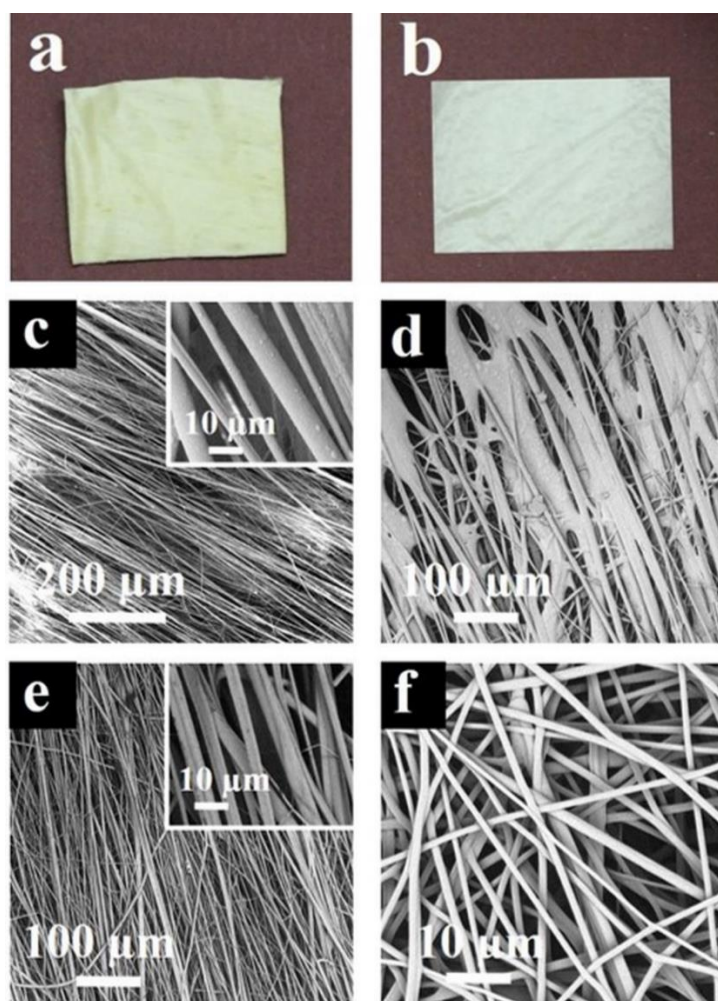


**Figure 5.3** Digital images of (a) PEF and (b) TLF; SEM images of PEF (c) and (d); SEM images of (e) TLF and (f) PSF

When the fibers were prepared using primary extract, then the middle and bottom layers (as explained in chapter 4) are also the part of fabrication process. The middle layer (ML) constitutes the solid particles present in peel and have the tendency to absorb TL

and BL, making it sticky in nature. Therefore, while drawing and depositing fibers, presence of ML can lead to merging of fibers, as shown in figure 5.3.d, in some places of mat obtained. This can be avoided if TL is used for drawing fibers. Electrospun PS fibers have diameter of about 500 nm and are randomly distributed as shown in figure 5.3.f.

### 5.3.2 Specific surface area (SSA) measurement

BET surface area of PEF was found to be 1.85 m<sup>2</sup>/g, which increases to 3.24 m<sup>2</sup>/g when only top layer is used to prepare fibers. The less surface area in case of PEF is attributed mainly due to the merging of fibers because of presence of sticky particles of middle layer. Surface area of electrospun PS fibers were found to be 50.01 m<sup>2</sup>/g. It is higher than PEF and TLF because of decrease in the fiber diameter on electrospinning.

### 5.3.3 FTIR/ATR Spectroscopy

The FTIR analysis of PS submicron fibers prepared by drawing i.e, PEF and TLF and electrospun PSF are shown in figure 5.4. The peaks at 1260 and 1280 cm<sup>-1</sup> show symmetric methylene stretching while bending vibration of out-of-plane C-H bonds of aromatic benzene ring were observed at 698, 756 cm<sup>-1</sup> respectively. Few other peaks at 601, 1493 and 1452 cm<sup>-1</sup> showed aromatic ring breathing modes of benzene ring in PS. Also 3082, 3061, 3027 cm<sup>-1</sup> were observed for the aromatic C-H stretches of benzene ring.

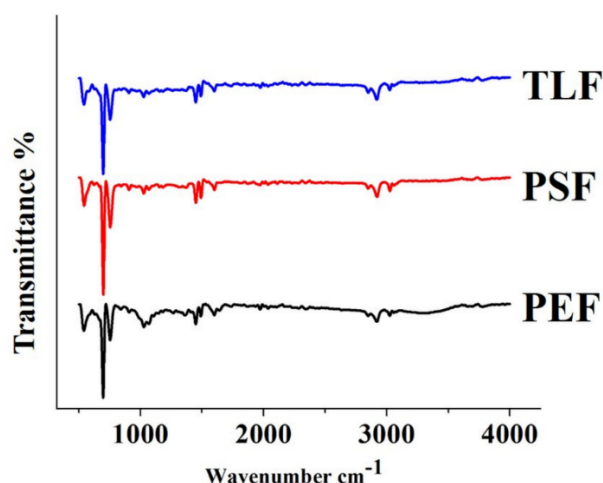


**Figure 5.4** FTIR analysis of TLF, PSF and PEF

The peak positions of PEF and TLF are identical to the electrospun PSF, therefore, it can be concluded that the geometric scale was successfully converted/recycled into fibers using orange peel extract.

### 5.3.4 X-ray diffraction analysis

The comparison of X-ray powder diffractions of drawn PEF and electrospun PSF revealed more evidently that the nature of both the fibers was almost same as shown in figure 5.5. Both the PEF and PSF showed broad amorphous peak at  $2\theta = 19.4^\circ$ .

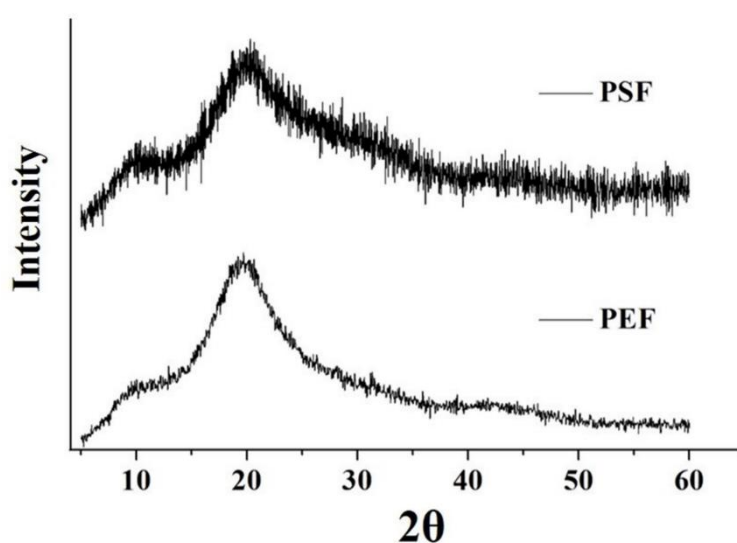


**Figure 5.5** XRD analysis of PSF and PEF

### 5.3.5 Contact angle measurement

Figure 5.6.a shows the optical image of water and oil droplet on prepared aligned PEF. As can be seen, water droplet is stable on fiber mat and makes an obtuse angle with fiber. But oil (mustard oil) was absorbed by the fibers. The PEF showed ultra-hydrophobicity with a contact angle of  $126.4 \pm 8.6^\circ$  (figure 5.6.b). Therefore, these fibers are hydrophobic and oleophilic in nature.

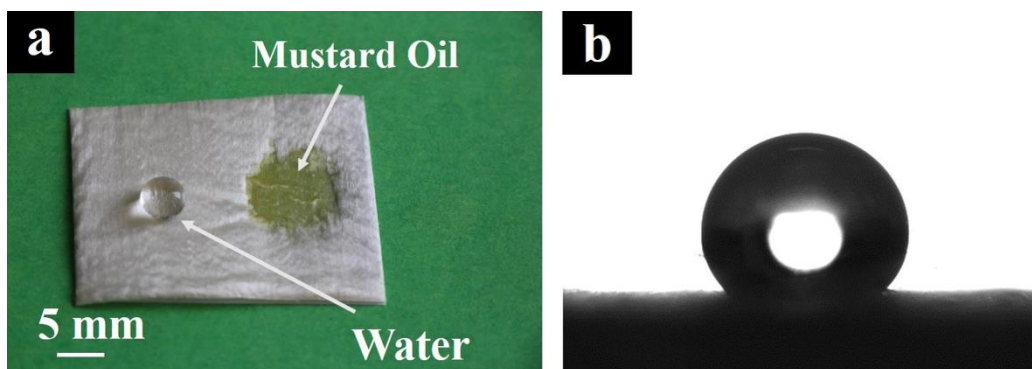


**Figure 5.6** (a) Optical image of water and oil droplet on as-drawn PEF and (b) contact angle on PEF

### 5.3.6 Thermogravimetric analysis

Figure 5.7 compares the thermal stability of PEF and TLF with electrospun PSF. In case of PEF, initial weight loss of 6.93% between 40 to 180 °C is due to the elimination of volatile components present in the mat. Second stage of weight loss, from 180 to 320 °C corresponds to thermal degradation of particles of ML present in PEF. The third stage of weight loss beyond 320 °C is due to the degradation of PS. In TGA of TLF, there are only two stages 40-280 °C and 280-400 °C corresponding to loss of volatile matter and degradation of PS respectively. In electrospun PSF, it degrades at about 300 °C to 0.6 wt% with zero char yield.

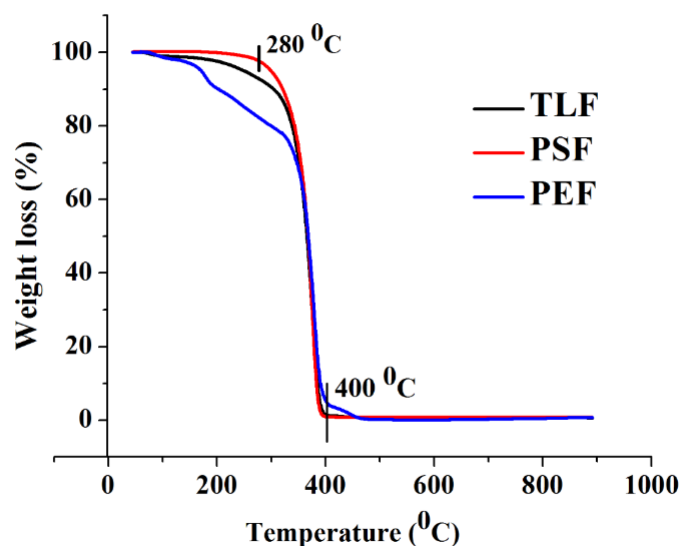


**Figure 5.7** TGA curve of TLF,PSF and PEF

### 5.3.7 Absorption capacity

Figure 5.8 illustrates oil absorption capacities of PEF and TLF and compares with the electrospun PSF. The absorption capacity of PEF mat for coconut oil and mustard oil is  $23.8 \pm 2$  g/g and  $12.9 \pm 1.8$  g/g respectively. When only top layer is used to make fibers i.e., for TLF, absorption capacity increases to  $30.7 \pm 0.4$  g/g to  $40.5 \pm 3.6$  g/g for coconut and mustard oil respectively. In the process of oil absorption, the coconut oil moves quickly and easily through the interior of fiber mat due to its less viscosity as compared to mustard oil. Therefore, both the fiber mat shows higher absorption for coconut oil.

In case of PEF, presence of particles of ML or merging of fibers restricts the movement of oil and as a result, the absorption capacity of PEF is 28.99% and 213.95% less than TLF for coconut and mustard oil respectively. Electrospun PSF had about  $58.80 \pm 2.6$  g/g absorption capacity for coconut oil and  $57.25 \pm 11.44$  g/g for mustard oil. The high oil absorption capacity of PSF is the result of high surface area due to decrease in the fiber diameter. It should be noted that though the absorption capacity of PEF and TLF is less than PSF but it has bright future in oil spill clean-up because the fibers have the advantage of being made by recycling PS along with using waste orange peel with very easy fabrication method.

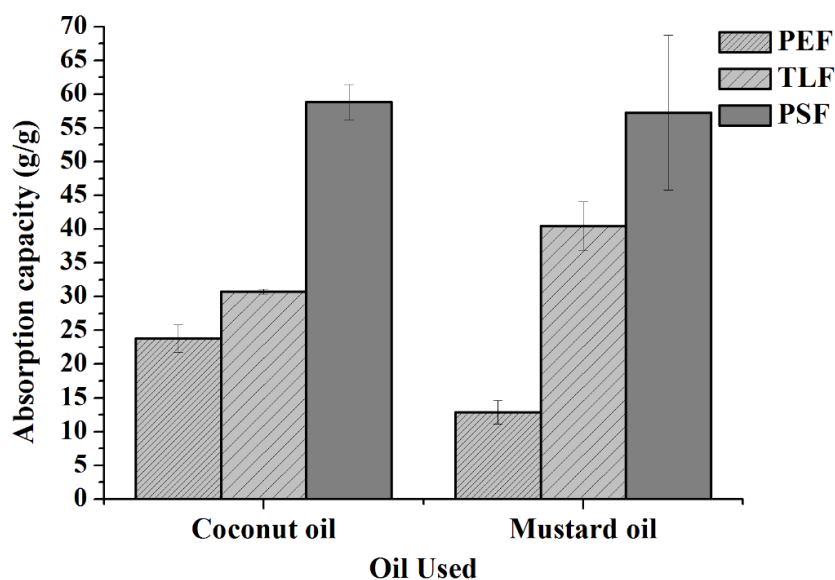


**Figure 5.8** Absorption capacity of PEF, TLF and PSF in coconut and mustard oil

### 5.3.8 Retention test

One of the most important property of sorbent material is its ability to retain the oil after absorption. Oil retention test was done to study the retention capacity of prepared



material against gravity with respect to time. Figure 5.9 represents rate of desorption of oil from PEF, TLF and electrospun PSF. In case of Coconut oil, there was sudden loss of oil from the sample in the first 10 min, i.e., absorption decreases to  $20.5 \pm 0.7$ ,  $26.8 \pm 0.1$  and  $46.7 \pm 2.4$  g/g for PEF, TLF and PSF respectively (figure 5.9.a). From the percent oil retention (figure 5.9.a'), percent loss of oil is about 13.8, 12.9 and 20.6% respectively for PEF, TLF and PSF in first 10min. After 1 hr, loss of oil is about 35.4% for PEF, 25.2% for TLF and 35.2% for PSF.

When the retention behaviour was studied with mustard oil, loss of oil in initial 10 min was found to be  $11.7 \pm 1.7$ ,  $31.5 \pm 1.2$  and  $47.2 \pm 7.6$  g/g for PEF, TLF and PSF respectively (figure 5.9.b). As can be seen from figure 5.9.b', this loss in weight is equivalent to 9.4% for PEL, 22.2% for TLF and 17.6% for PSF. After 1 hr, PEF, TLF and PSF fibers still retained 77.3, 59.9 and 66.3% of mustard oil respectively.

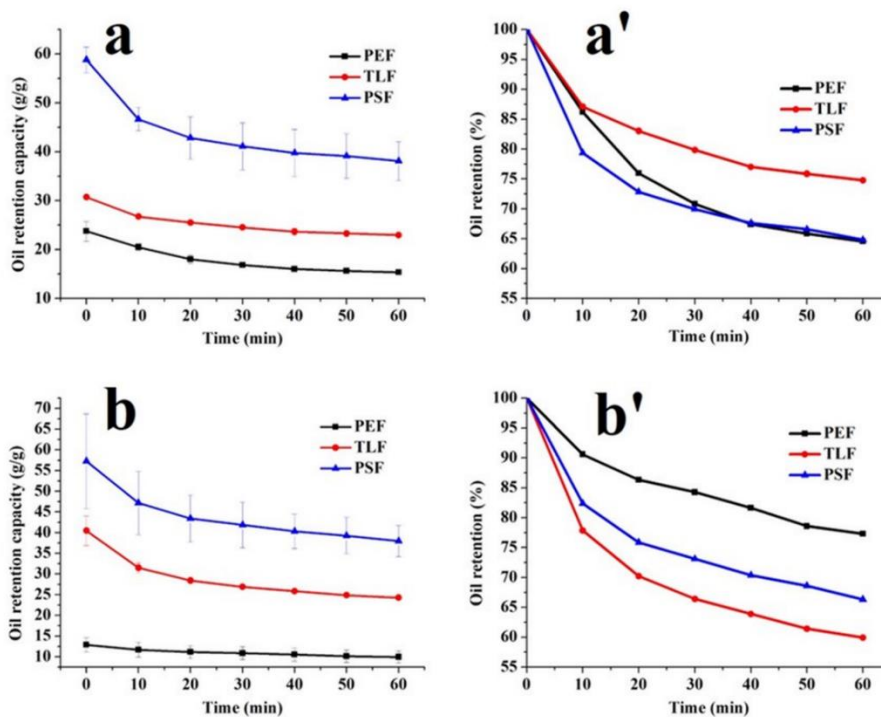


**Figure 5.9** Oil retention capacity of PEF, TLF and PSF in (a) coconut oil (b) mustard oil and respective percent retention (a' and b')

### 5.3.9 Reusability test

The efficiency of sorbent material if it can be reused multiple times. Therefore, reusability test was done to know the absorption capacity of fibers after certain number

of cycles. Figure 5.10 represents the comparisons in the absorption capacity of PEF and TLF in coconut and mustard oil for first and fifth cycle respectively.

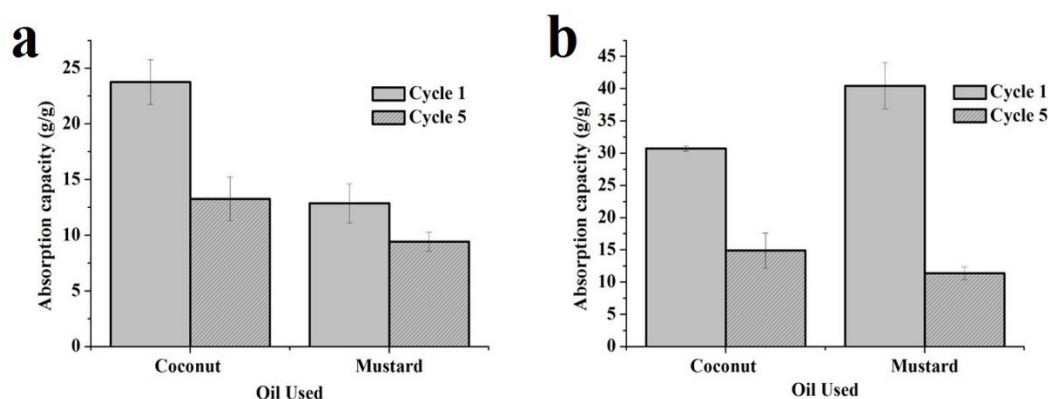


**Figure 5.10** Reusability of (a) PEF and (b) TLF in coconut and mustard oil

In case of PEF, for coconut oil, the absorption capacity decreases from  $23.8 \pm 2$  g/g to  $13.2 \pm 1.9$  g/g and for mustard oil, its decrease is from  $12.9 \pm 1.8$  g/g to  $9.4 \pm 0.8$  g/g. This decrease in the absorption capacity is mainly attributed to the decrease in the pore size or change in the morphology on compressing to squeeze out the oil from sample. Similar trend was obtained in case of TLF. Absorption capacity decrease to  $14.9 \pm 2.7$  g/g and  $11.4 \pm 0.9$  g/g from  $30.7 \pm 0.4$  g/g and  $40.5 \pm 3.6$  g/g for coconut and mustard oil respectively.

### 5.3.10 Buoyancy test

After absorption of oil, fibres should not sink in the water body as a result of increase in weight of sample. Therefore, buoyancy test was done to check the buoyancy in both static and dynamic system. The sorbent will float on water surface before and after absorption if buoyancy is high. In static system, figure 5.11a-c, PEF sample floats on the surface and keeps on sucking oil. After 30min PEF absorbs all mustard oil and still floats on surface (figure 5.11a-c).

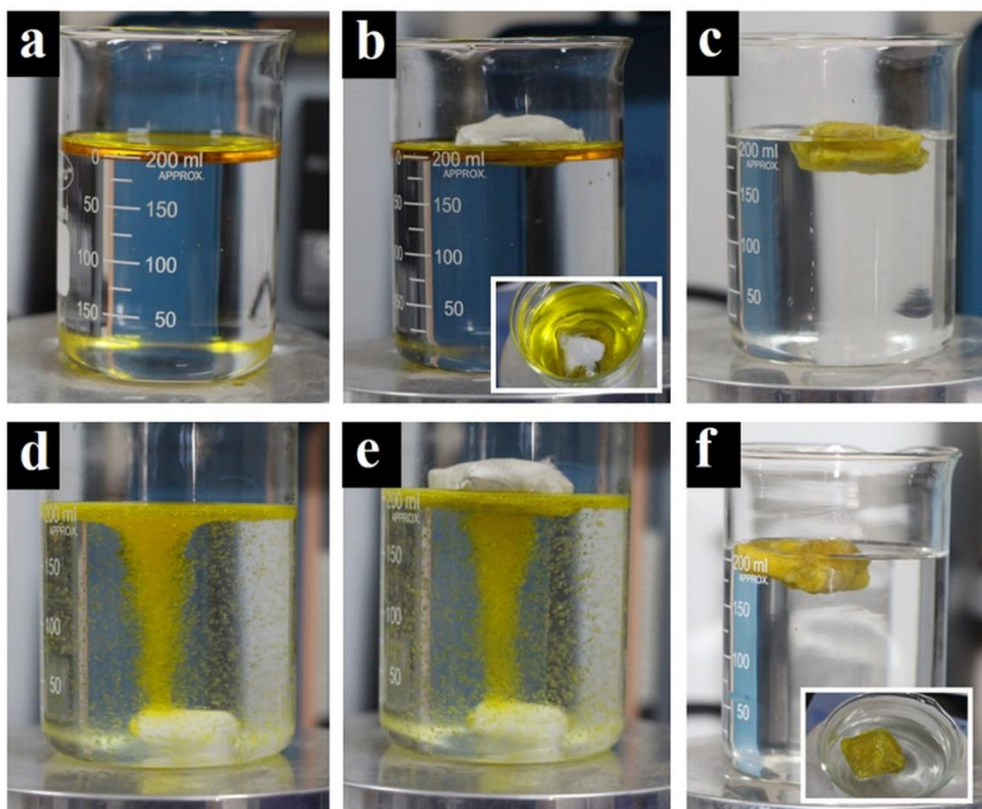


**Figure 5.11** Clean-up of mustard oil by PEF in static system (a-c) and dynamic system (d-f)

Similarly in dynamic system, though there is continuous stirring (figure 5.11d), sample floats after absorption of oil (figure 5.11e-f). Therefore, PEF shows high buoyancy, mainly due to its hydrophobic and oleophilic nature.

#### 5.4 Conclusions

The geometric scale and thermocol, made up of Polystyrene was successfully converted into sub-micron, aligned fibers with controllable geometry, used orange peel extract. The process used is very flexible and needs minimum equipment. The fibers produced were then characterised in terms of surface morphology, crystal size, surface area, thermal stability and wettability behaviour. The fibers were found to be hydrophobic and oleophilic in nature. Based on this property, these fibers were then tested as a sorbent material for oil. These fibers showed good absorption and retention capacity. Also they withstand upto 5 cycles of reusability without tearing and were found to have high buoyancy. These fibers have great potential to be used as sorbent material for oil.

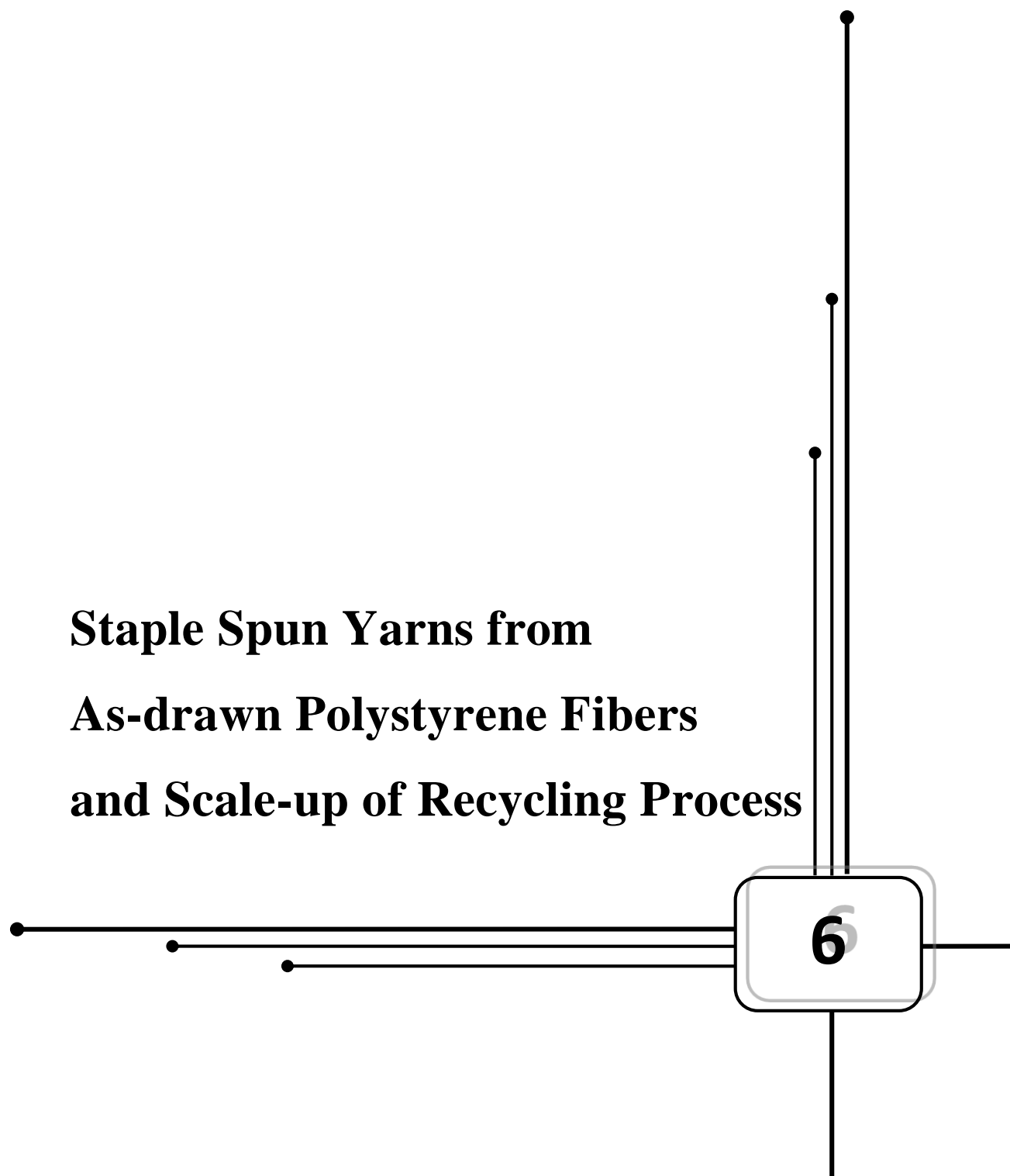
## **5.5 Acknowledgements**

We acknowledge Dr(s). Prabu Sankar and Dr. Atul Deshpande and for their help in FTIR/ ATR and BET analysis. We also acknowledge help and valuable suggestions from Mrunalini Gaydhane and Srinadh Mattaparthi.

## References

1. A. Azapagic, A. Emsley, I. Hamerton. *Polymers, The Environment and Sustainable Development*, John Wiley & Sons Ltd, England 2003
2. Website. <http://pr.hec.gov.pk/chapters/827s-1.pdf>
3. T. Maharana, Y. S. Negi, B. Mohanty. Review Article: Recycling of Polystyrene, *Polymer-Plastics Technology and Engineering*, 46 (2007), 729-736
4. H. Zhu, S. Qiu, W. Jiang, D. Wu, C. Zhang. Evaluation of Electrospun Polyvinyl Chloride/Polystyrene Fibers As Sorbent Materials for Oil Spill Cleanup, *Environ. Sci. Technol.*, 45 (2011), 4527–4531
5. J. Lin F. Tian, Y. Shang, F. Wang, B. Ding, J. Yu and Z. Guo, Co-axial electrospun polystyrene/polyurethane fibres for oil collection from water surface *Nanoscale*, 5 (2013), 2745–2755
6. C. Shin, G. G. Chase. Nanofibers from recycle waste expanded polystyrene using natural solvent, *Polymer Bulletin*, 55 (2005), 209–215
7. M. T. García, I. Gracia, G. Duque, A. de Lucas, J. F. Rodríguez, Study of the solubility and stability of polystyrene wastes in a dissolution recycling process, *Waste Management*, 29 (2009), 1814–1818

**Staple Spun Yarns from  
As-drawn Polystyrene Fibers  
and Scale-up of Recycling Process**



## **Abstract**

The textiles has been used worldwide in impressive number of applications such as decorative fabric, climate control garments, protective clothing, medical fabric, electronic textile, military etc. Fibers are generally converted into yarns and therefore used for making multitude products such as, woven fabrics, towels, carpets, etc. The fabric properties are mainly dependent on fiber properties, fabric and yarn structure. In this work, we attempt to convert the as-drawn polydyrene (PS) fibers into yarns and coils. These coils were than tested in terms of surface morphology using scanning electron microscope (SEM) and strength by making different knotted structures such as square, overhand and weaver's knot.

Further, we illustrate the drawing of fibers from waste PS using a simple prototype developed based on hydraulics and replacing operators hand with suitable material for scale up.

## **6.1 Introduction**

Textiles have been used for centuries to meet apparel and domestic needs<sup>1</sup>. Nowadays, technical usage of textiles has been growing and therefore referred as technical textiles<sup>1</sup>. Apart from use in traditional and home, textiles are used in areas such as healthcare, safety, electronics etc. Yarns are the basic building blocks of most of these textile forms or fabrics<sup>2</sup>. Fibers are generally converted into yarns and therefore used for making products such as, woven fabrics, towels, carpets, etc. A staple –spun yarn is linear assembly of many fibers in the cross section and along the length, held together usually by the insertion of twist to form a continuous strand, small in diameter but of any specified length. It is used for interlacing in processes such as knitting, weaving and sewing<sup>2</sup>. The fabric properties are mainly dependent on fiber properties, fabric structure and structure of yarns.

This work is an attempt to convert the as-drawn PS fibers (as mentioned in chapter 5) into yarns and coils. The morphology of prepared yarns and coils was then checked under scanning electron microscope (SEM). These coils were then tested by making different knotted structures such as square, overhand and weaver's knot as in processes such as winding, weaving, sewing, wrapping etc. two ends of the yarns or coils are connected by making knots<sup>2</sup>. The drawing method used for recycling waste PS objects into aligned sub-micron fibers have the advantage of being handy, inexpensive and minimum equipment requirement. However, this method involves operator's hand as the surface for attaching fibers and limits the applications. Therefore, it needs modification in order to scale the fiber production for application such as oil spill remediation, yarn or coils in textile etc. Therefore, we search for suitable material for replacing hand in the process and also illustrates simple set-up based on hydraulics.

## **6.2 Experimental method**

### **6.2.1 Materials**

PEF membranes (as prepared in chapter 4). Geometric scale, eraser, 10mL syringes, water pipe and thermocol were purchased from local market.

### **6.2.2 Hand-spun yarn and coil**

The recycled PS fibers (i.e., PEF or TLF) were twisted into yarn as shown in figure 6.1. The PEF membrane was cut into ribbons and was twisted from one end as represented in fig. 6.1.a-



c. After certain twists into ribbon, yarn was obtained (figure 6.1.d). If the yarn was over twisted, it starts converting into coil (fig. 6.1.e).

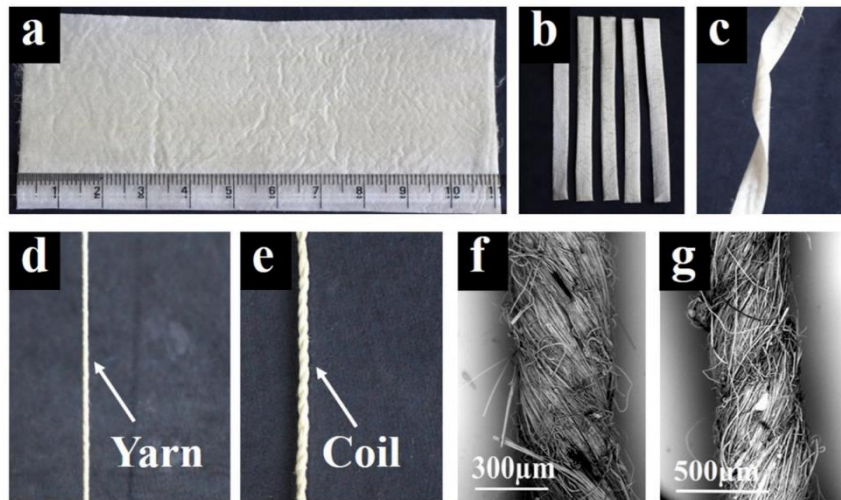


**Figure 6.1** Steps in making yarn and coil (a-e); SEM images of (f) yarn and (g) coil

### 6.2.3 Knot test<sup>3</sup>

In processes such as winding, weaving, sewing, wrapping etc. two ends of the yarns or coils are connected by making knots. Some of the knots were tried using the coils produced above such as square, overhand and weaver's knot as shown in figure 6.2.a-c.

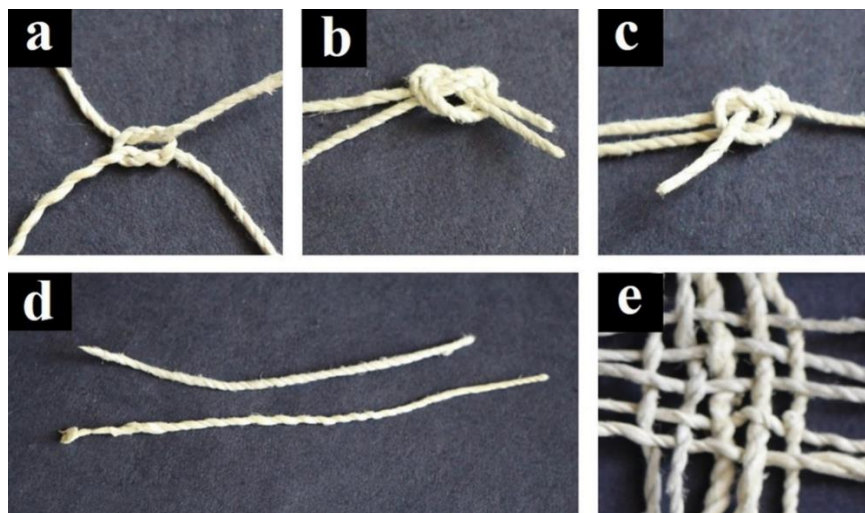


**Figure 6.2** Knotted structures (a) square, (b) overhand and (c) weaver's knot; (d) coils after opening knot and (e) weaving different diameter coils.

### 6.2.4 Material for the process

As mentioned earlier, we need suitable material to replace operator's hand from the drawing method. The properties of hand or material properties needed for this process are as follows:

1. The material should not react with the primary extract of the orange peel.
2. It should provide sufficient roughness to stick fibers on the surface.
3. It should be flexible and soft as our hand, while pressing PS objects to it (as illustrated in chapter 5).

It has been found that the commercial erasers satisfies all the requirements mentioned above. Therefore, figure 6.3 represents the recycling of scale using eraser in place of hand. The steps involved are:

1. Squeezing orange peel on scale (figure 6.3.a)
2. Take eraser/rubber in place of hand (figure 6.3.b)
3. Press eraser/rubber on scale (figure 6.3.c)
4. Drawing fibers by horizontally outwards (figure 6.3.d) and following steps as mentioned in previous chapter.

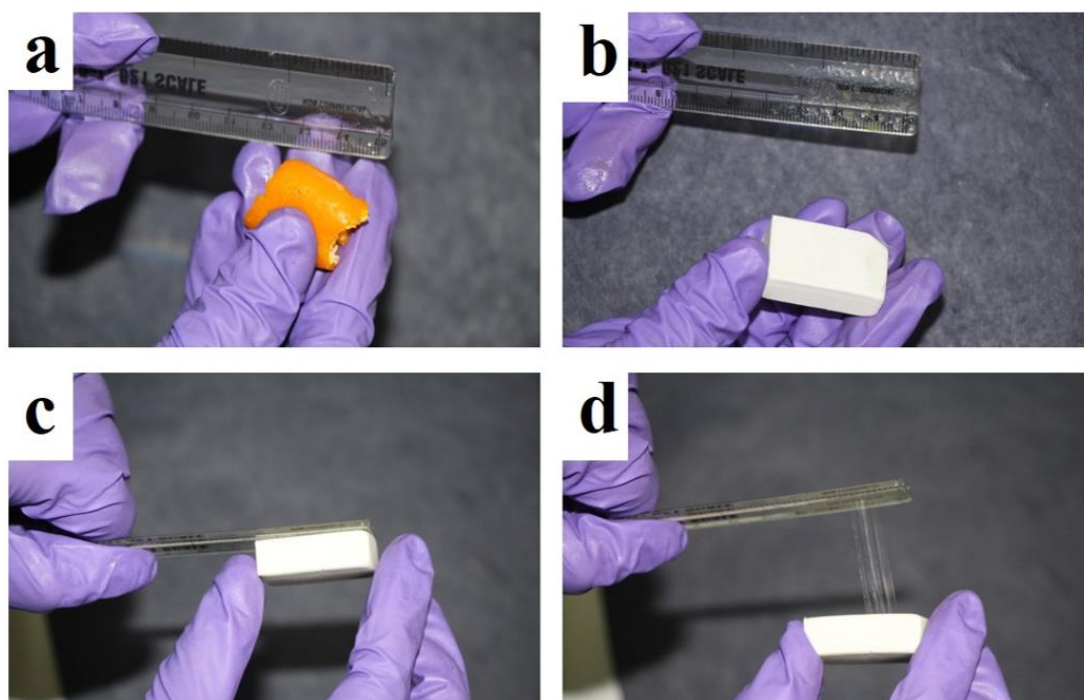


**Figure 6.3** Use of eraser for fabricating fibers

### 6.2.5 Set-up for drawing method

Figure 6.4.a represents the set-up for drawing of fibers from waste PS. Syringes with water pipes are used for giving movement to eraser and collector. Geometric scale is fixed approximately 10 cm in front of eraser. Similarly, collector attached to one of the syringe is placed besides eraser and perpendicular to gap between scale and eraser.

## **6.3 Results and Discussions**

### **6.3.1 Morphological Characterization**

Figure 6 also represents the SEM images of yarn and coil. The outer diameter of yarn produced is about 350-400  $\mu\text{m}$  and for coil it is approximately 500-600  $\mu\text{m}$  as shown by the SEM images of yarn and coil in fig. 6.1.f and 6.1.g respectively.

### **6.3.2 Knot test**

The knotted structure were successfully prepared, as shown in figure 6.2. When these knots were opened, there was no breakage in the coil (figure 6.2.d), therefore, these can be reused. Figure 6.2.e represents an example of weaving coils.

Therefore, yarns and coils were successfully prepared using hand-spinning. These can be further used for weaving, sewing etc. Moreover, as the material of fibers was PS, these yarns and coils have following advantages:

1. They are hydrophobic. Therefore, can be used to get water or stain-resistant fabrics.
2. Oleophilic and therefore can be used as filtrate medium for separating oil from water.
3. They are electric insulators and therefore can be used for making gloves, warm clothing, protective clothing etc.
4. Ease in fabrication and cost effective method along with recycling waste PS using waste orange peels.

### **6.3.3 Scale-up of fabrication process**

After selecting eraser as the material for drawing fibers from PS objects, next step is to reduce manual efforts.

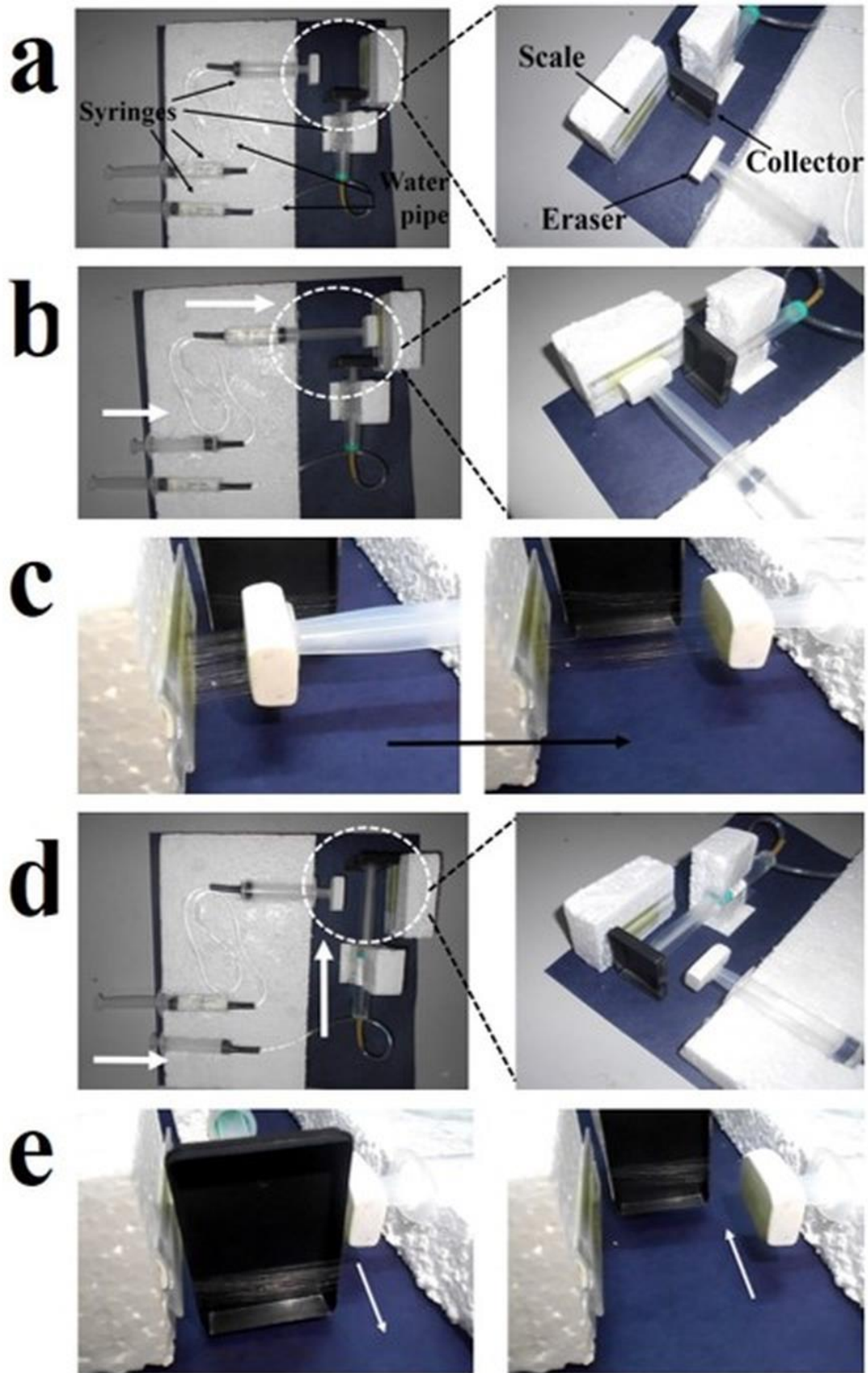


**Figure 6.4** Digital images of steps of working set-up prototype.

Figure 6.4 represents the set-up and steps are as mentioned below:

1. Put few drops of top layer or primary extract on the scale and place it in front of the eraser (figure 6.4.a)
2. As the syringe at the centre is moved forward, the piston with eraser moves towards scale. Continue pushing piston till the eraser touches scale (figure 6.4.b)
3. When the direction was reversed, eraser moves horizontally outward and fibers can be seen as in figure 6.4.c.
4. These drawn fibers were then deposited on collector. For that, the other syringe's piston was moved inward, resulting in the movement of collector, perpendicular to fiber direction (figure 6.4.d)
5. Figure 6.4.e shows the fiber breakage by collector edges and its backward movement.
6. Repeat steps 2-5 till the solution dries and then repeat step 1.

Therefore, the drawing of fibers from waste polystyrene objects using hand was successfully done using simple hydraulics. Further, the movement of pistons can be made fully automated using electric motors etc.

#### **6.4 Conclusions**

Yarns and coils were fabricated by hand-spinning from as-drawn polystyrene fibers prepared by using orange peel extract. The yarns and coils were found to have an outer diameter of about about 350-400  $\mu\text{m}$  and 500-600  $\mu\text{m}$  respectively. These can be used for weaving or making knotted structures and can also be reused. Further, we successfully replicated drawing of PEF using set-up based on hydraulics. Therefore, production of fibers can be scaled up, enabling us to explore more applications using this process and fibers.

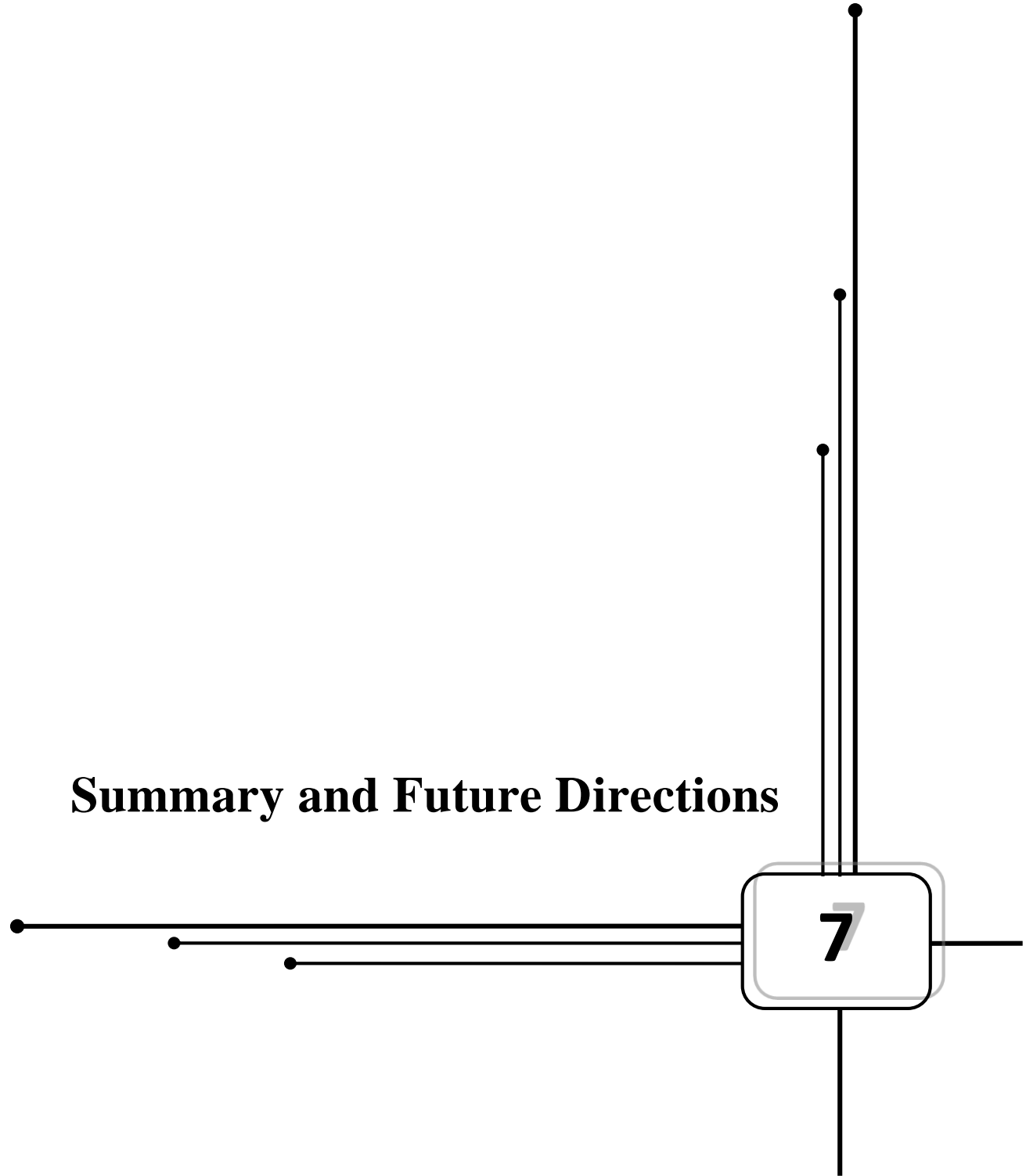
#### **6.5 Acknowledgements**

We would like to thank Dr. Mudrika Khandelwal, Mrunalini Gaydhane and Srinadh Mattaparthi for their help and suggestions for this work.

## References

1. R. Chattopadhyay, Introduction: types of technical textile yarn in Technical Textile yarns, Woodhead Publishing Limited, 2010
2. C. A. Lawrence, Overview of developments in yarn spinning technology, Woodhead Publishing Limited, 2010
3. D. Petrulis, S. Petrulyte, Tensile properties of knotted line flax spun yarns, *Fibres & textiles in Eastern Europe*, 20 (2012), 48-53.

# Summary and Future Directions



## **7.1 Summary**

This work was intended to explore various applications of submicron- and nano-fibers from different polymers. The biopolymers such as cellulose acetate and gelatin were successfully electrospun. Depending on the application, these fibers were modified by encapsulating super absorbent polymer and piperine drug in cellulose acetate and gelatin nanofibers respectively. Further, different characterization were carried out to study morphologies, wettability behavior, thermal stability, drug release, absorption capacity etc. as per the requirement.

A very simple and novel method was developed to prepare orange peel extract, which is used without separation of components. This extract was then used for print transfer on different substrates and for recycling waste polystyrene objects into fibers. The as-drawn fibers were used as sorbent material for oil absorption and tested for textiles by converting into yarns and coils.

## **7.2 Future directions**

Based on the findings of thesis, some possible future directions are suggested briefly in this section. The basic idea is to extend the domain of this thesis. For example, in feminine hygiene application, anti-bacterial drugs can be encapsulated in cellulose acetate electrospun nanofibers. This can be helpful in preventing infections, skin allergies etc. by killing bacteria or inhibiting their growth.

It is well known that Piperine drug is used as a bio-enhancer for anti-cancer drug i.e., curcumin. Therefore, the use of gelatin as drug carrier can be extended by optimizing parameters for encapsulating curcumin in gelatin nanofibers. This combination of gelatin-piperine and gelatin-curcumin can be used together in form of multilayers or co-axial nanofibers, thereby enabling us to maximize the efficacy of drugs with minimum dosages.

The work of recycling waste polystyrene objects into sub-micron fibers can be industrialized by making suitable modifications in the set-up as introduced in chapter 6. The applications of these as-drawn fibers can be further explored.